Vibro-Acoustic Design Optimization Study to Improve the Sound Pressure Level

Inside the Passenger Cabin

by

Erdem Yüksel

A Thesis Submitted to the

Graduate School of Engineering

in Partial Fulfillment of the Requirements for

the Degree of

Master of Science

in

Mechanical Engineering

Koc University

April 2010

Graduate School of Sciences and Engineering

This is to certify that I have examined this copy of a master's thesis by

Erdem Yüksel

and have found that it is complete and satisfactory in all respects,
and that any and all revisions required by the final
examining committee have been made.

Committee Members:

_____

Ipek Başdoğan, Ph. D. (Advisor)

_____

Murat Sözer, Ph. D.

_____

F.Sibel Salman, Ph. D.

Date: _____

ABSTRACT

The interior noise inside the passenger cabin of automobiles can be classified as structure-borne or airborne. In this study, we investigate the structure-borne noise, which is mainly caused by the vibrating panels enclosing the vehicle. Excitation coming from the engine causes panels to vibrate at resonance frequencies which leads to change in the sound pressure level (SPL) in the passenger cabin .Two methodologies were used to predict the SPL inside the vehicle cabin. The Finite Element Method (FEM) was used for structural analysis of the vehicle, and Boundary Element Method (BEM) was integrated with the results obtained from FEM for acoustic analysis of the cabin. The adopted FEM-BEM approach can be utilized to predict the SPL and also to determine the contribution of each panel to interior noise. The design parameters of the most influential radiating panels (i.e., thickness) can be optimized to reduce interior noise based on performance metrics. A structured parametric study, based on techniques from the field of industrial design of experiments (DOE) was employed to understand the relationship between the design parameters and the performance metrics. A DOE study was performed for each metric to identify components that have the highest contribution to SPL and then regression models are built. Then, preliminary optimization runs are employed to improve the interior noise by finding optimum configurations for thicknesses. Our results show that

the methodology developed can be used for improving the design of panels to reduce interior noise when vibro-acoustic response is chosen as performance criteria.

ÖZET

Araç sürücü kabinindeki ses, yapıdan kaynaklanan ve havadan kaynaklanan ses olmak üzere ikiye ayrılır. Bu çalışmada, aracı çevreleyen panellerin titreşmesi nedeniyle oluşan yapıdan kaynaklanan ses türü araştırılmıştır. Motordan gelen tahrik, panellerin rezonans frekanslarında titremesine neden olmakta ve bu titreyen paneller kabin içinde ses basınç seviyelerinde değişikliğe sebep olarak istenmeyen ses türünü ortaya çıkarmaktadır. Motordan gelen tahrikin etkisi altında kabindeki ses basınç seviyelerini incelemek için iki farklı yöntemin birleşimi kullanılmıştır. Bu yöntemler, yapısal model için Sonlu Elemanlar Metodu (FEM)ve akustik model için Sınır Elemanlar Metodudur (BEM). Birleşik FEM-BEM metodu araç sürücü kabini içindeki ses basınç seviyesini ve ayrıca her panelin titreşiminin ses basıncına olan katkısını tahmin etmekte de kullanılabilinir. Daha sonrasında ses basıncına en çok katkısı olan panellerin tasarım parametreleri, belirlenen performans metrikleri esas alınarak ses basıncını azaltmak için optimize edilebilinirler. Tasarım parametreleri ve performans metrikleri arasındaki ilişkiyi anlayabilmek için endüstriyel deney dizaynı (DOE) dalındaki teknikler esas alınarak yapısal parametrik bir çalışma yürütüldü.

Araç kabini içindeki ses basıncına en çok katkısı bulunan bileşenleri bulmak için DOE çalışması gerçekleştirildi.Her bir analizde, bütün sistemin vibro-akustik analizi gerçekleştirldi, ses basınç değerleri motor devrine bağlı bir fonksiyon olarak hesaplandı ve her bir performans metriği elde edildi. Her bir performans metriği için ses basıncına en yüksek katkısı olan dizayn parametreleri belirlendi ve regresyon modelleri oluşturuldu. Kabin içi ses basıncını iyileştirmek için gerekli optimum panel konfigürasyonunu bulmak için optimizasyon çalışmaları gerçekleştirildi. Elde ettiğimiz sonuçlar gösteriyor ki; bu çalışmada geliştirilen method vibro-akustik tepki performans kriteri olarak ele alındığında , kabin içi sesi azaltmak için panel dizaynında kullanılabilinir.

ACKNOWLEDGEMENTS

TABLE OF CONTENTS

LIST OF TABLES

LIST OF FIGURES

NOMENCLATURE

$[K_a]$	Acoustic stiffness matrix
$[M_a]$	Acoustical mass matrix
$[Ca]$	Acoustical damping matrix
$[M]$	Structural mass matrix
$[K]$	Structural stifness matrix
$[C]$	Structural damping matrix
ω	Natural frequencies of the structural Model
p	Sound Presure
ATV	Acoustic transfer vector
ATM	Acoustic transfer matrix
$MATV$	Modal acoustic transfer vector
w	Nodal displacements of the panels
$MPSP$	Vector of the modal participation factor

Chapter 1

INTRODUCTION

1.1 Overview

The reduction of vehicle interior noise has become one of the most important issues related to driving conveniences. Vehicle interior noise is usually quantified by sound pressure level (a.k.a., sound level), which is a logarithmic measure of the sound pressure of a sound relative to a reference value. Sound pressure level is measured in decibels (dB). The commonly used reference sound pressure in air is $p_{ref} = 20$ µPa, which is usually considered to be the threshold of human hearing. However, for automotive applications, frequency weighted, dB(A) measure is used to approximate the human ear's response to sound using the A-weighted scale [1].

Sound pressure level varies as a function of the speed of the vehicle's engine. There are many sources that may cause the sound pressure level to increase inside the passenger

cabin. These sources can be classified as structure-borne and airborne [2]. In this study, we investigate the structure-borne noise, which is mainly caused by the vibrating panels enclosing the vehicle. The excitation coming from the engine may cause these panels to vibrate, and consequently, cause an increase in the sound pressure level. The increase in the sound pressure level generally corresponds to an undesirable booming noise, which is usually felt in the low frequency range of 50-200 Hz inside the passenger cabin. In order to reduce the interior noise, it is critical to understand the dynamics of the vehicle, and more importantly, how it interacts with the air inside the cabin. The objective of the present study is to demonstrate a methodology that can be used to identify the key contributors to structure-borne vibration induced interior noise in a commercial vehicle and reduction of the noise levels through optimization. A generalized methodology was developed for defining the optimal relationship among the panel design parameters and vibro-acoustic performance of the vehicle.

For the vibro-acoustic study, mainly two simulation methods, which are Finite Elements Method (FEM) and Boundary Elements Method (BEM) are used. Chapter 3 presents the details of the uncoupled method and the details of the combined FEM/BEM approach to identify the sound pressure level inside the passenger cabin. Many researchers have studied and reported on the accuracy and limitations of both of these methods. For example, structural vibro-acoustic analysis of vehicles, in which both FEM and BEM have

been used, was reported in the studies [3, 5]. In these papers, the vibro-acoustic response of vehicle using either a strongly coupled structure-fluid interaction method or an uncoupled structure-fluid interaction have been investigated and discussed in great detail. Suzuki et al. [3] performed BEM to overcome the noise problems inside a vehicle cabin. They studied the effect of absorbent materials adhered to vibrating surfaces to prevent air leakage from the cabin walls. In Pal and Hagiwara's study [5], FEM was performed for the coupled structure-fluid problems. They analyzed the correlation between vibration of cabin walls as well as the sound pressure level at the position of the passenger ear. Liu et al. [6] created a vibro-acoustic model to predict the noise inside the tracked vehicles. They determined the interaction forces in the vehicle by using the ADAMs software. In their study, both FEM and BEM models were used for the vibro-acoustic analysis. Kim and Lee [7-8] made studies about the acoustic/structural coupling. Their studies involve the structural-acoustical response of a vehicle compartment in terms of the structural-acoustic modal coupling coefficients. Moreover they also investigated the contribution of the structural panels to the interior noise levels inside the passenger cabin.

Freymann et al. [9] focused on the coupled systems and investigated fluid-structure interaction to predict the sound pressure levels for coupled systems. Finite element (FE) and boundary element (BE) models of the chassis hull of the vehicle were created and adopted to perform the vibro-acoustic analysis. In a similar study by Paul and Hagiwara [10], the correlation between vibration of cabin walls and sound pressure level at the ear of

the vehicle driver was analyzed using FE methods. Marburg and his co-workers [11-15] investigated the vibro-acoustic response of the noise level inside the vehicle cabin and also developed techniques to optimize the design parameters based on the vibro-acoustic analysis. Bregant et al. [16] modeled a 3D cavity representing the earth-moving machine cab in ANSYS. They performed A BEM coupled analysis in Virtual Lab to evaluate the cab vibro-acoustic field. They also modified the structural parameters based on the results of a vibro-acoustic field optimization. Desmet and Vandepitte [17] described the use of finite element method for time harmonics acoustic problems. Besides the basic principles of finite element method, they proposed some mathematical definitions for an interior acoustic problem. Desmet [18] has another paper that focuses on the boundary element methods which is another valuable technique for vibro- acoustic problems. Herrin et al. [19] focused on Acoustic Transfer Vector (ATV) which enables the contribution analyses to identify the problem sources. They studied on an engine model which is separated into several different components. The objective of this study, which is based on the contribution analysis, is to understand how these different sound radiating components contribute to the overall sound pressure level, and also to find out the reason for their low or high contribution.

In this study, we adopt a combined use of FEM and BEM methodologies in order to predict the sound pressure level inside the passenger cabin of a commercial vehicle. We

choose uncoupled analysis approach for the vibro-acoustic analysis. We use FEM for the structural analysis and BEM for the acoustic analysis. The adopted FEM-BEM approach takes advantage of the Acoustic Transfer Vectors (ATV) to calculate the sound pressure levels at the predefined locations as a function of engine speed. ATVs are transfer functions that link the structural vibrations of the radiating surfaces and the sound pressure levels at the desired output field points. The contribution of each radiating panel to the interior noise is calculated using Panel Acoustic Contribution Analysis (PACA) . PACA takes advantage of the ATVs and enables the user to identify the most critical radiating panels. This information can then be utilized to reduce the cabin noise by focusing on these critical panels.

Although the results of the PACA contains a lot of useful information, it does not provide any guidance to the designer regarding how these panels should be modified so that the sound pressure levels can be reduced. The PACA results are only based on the current design and they do not provide any information regarding how the performance changes if any or all of these panel design variables are changed within a certain range. The vehicle contains many structural panels and consequently, there are many design variables that should be looked at when a redesign effort is considered. Especially, when the coupling between the structure and cavity and the interactions between the panels are considered, the reduction of sound pressure level forms a highly non-linear optimization

problem, and hence is still considered to be a complicated task even for a simple vibro-acoustic problem.

Considering all these needs, we employ techniques from the fields of Design of Experiments (DOE) to understand the relationship between the studied design parameters and sound pressure level. The PACA results are chosen as the basis for the DOE study. The thicknesses of the same panels used in the PACA are used in a DOE study to identify the important ones. Following the DOE analysis, response surfaces are built to be used for the optimization studies. Preliminary optimization studies are employed using the regression models generated in the Response Surface Method (RSM) study. Chapter 2 gives the details of the vibro-acoustic model that was used in this study. The details of the DOE study and the construction of the regression models are given in Chapter4. The results of the preliminary optimization studies are explained in detail in Chapter 4.

1.2 The Contributions of this Thesis

In this thesis, a systematic methodology for predicting the interior noise level of a commercial vehicle under the effects of engine disturbances is presented. The methodology presented in this thesis also identifies the problematic components and panels of the vehicle that contribute to the SPL at most.

The interior noise of the passenger cabin of a commercial vehicle is used as the case study to demonstrate the developed methodology. A generalized methodology for defining

the optimal relationship among the panel design parameters and vibro-acoustic performance of the vehicle is presented.

One of the most important contribution of this thesis is the "emphasize of the performance metrics." In this thesis our study shows that the performance metric selection is also very critical in terms of defining the optimum solution and also finding the optimized configuration.

CHAPTER 2

THEORY OF VIBRO-ACOUSTIC ANALYSIS

2.1 Overview

This chapter presents the details of the uncoupled vibro-acoustic analysis that are used in investigation of sound pressure levels (SPL). Finite element method (FEM) and Boundary element method (BEM) are used for modeling the structural model and acoustical cavity to perform the vibro-acoustic analyses [1, 2]

One of the most common methods which is used in engineering applications is the finite element method (FEM). In Finite Element Method, the problem is derived into an equivalent integral formulation. Then, the variable distribution and the geometry of the domain is approximated in terms of shape functions. These shape functions are defined within the small subdomains called "finite elements" of the continuum domain. Therefore, the original problem for a continuum domain is transformed into a problem of some nodal positions within each element, thus transformed into a set of algebraic equations[3].

Coupled and uncoupled FE analyses are generally used to predict the SPL of the vehicle due to the engine disturbances. The *uncoupled vibro-acoustic analysis* does not

consider the mutual coupling interaction between the structural and the fluid components. However, in the *coupled vibro-acoustic analysis* approach, the mutual vibro-acoustic coupling interaction between the structural and fluid components is no longer negligible and the system is treated as a coupled system. When the interaction between the vehicle structure and the cabin interior acoustics is studied, only one way interaction can be considered and these type of problems are usually treated as uncoupled systems. For that reason, we used the uncoupled approach for our vibro-acoustic analysis to predict the SPL inside the passenger cabin.

In the previous studies G.Kamçi et al [4]; investigated the interior noise level of the passenger cabin both comparing the results of the coupled and uncoupled analysis with the obtained experimental results acquired from the company.

As seen from figures 2.1 and 2.2, the results did not change significantly when those two methods were compared which gave an indication that the effect of the fluid on the structure can be neglected.

At the position of driver's left ear
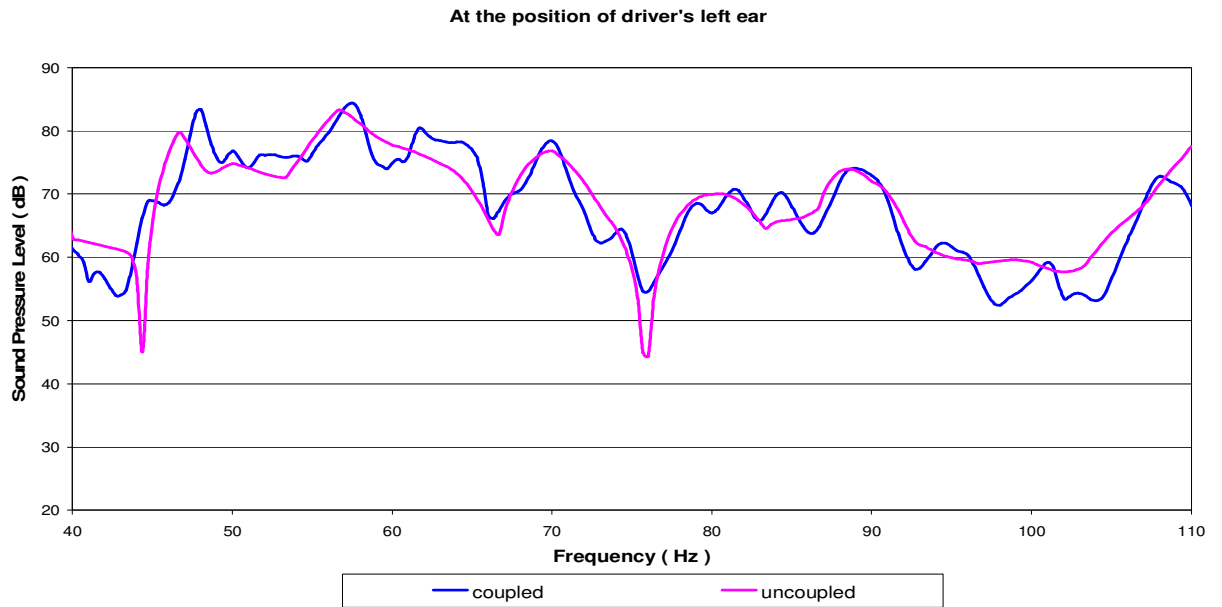
Figure 2.1: Comparison of the results of two methods (coupled & uncoupled) at the position of left ear of the driver.

At the position of driver's right ear
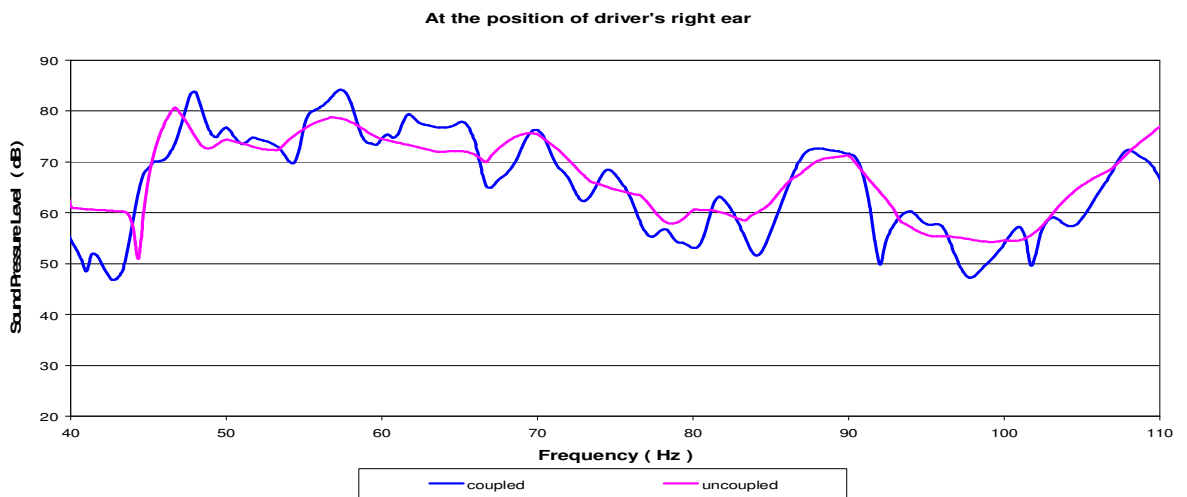
Figure 2.2: Comparison of the results of two methods at the position of right ear of the driver
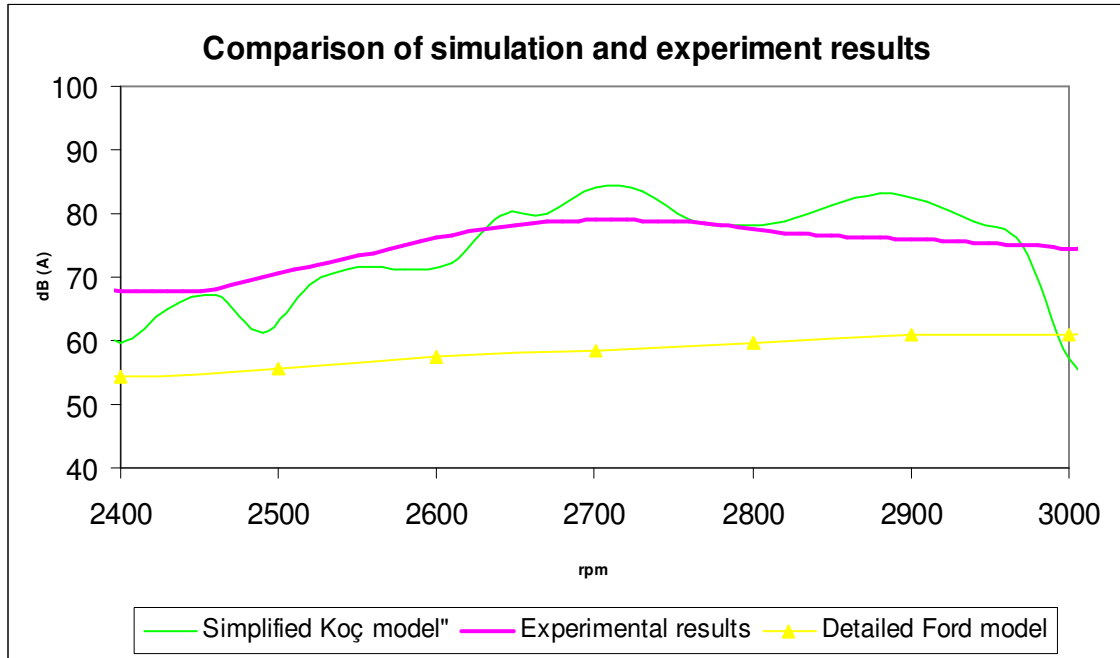
Figure 2.3 : Simulation results of the analyses performed at Ford Otosan and LMS Virtual Lab.

The structural model which is used in all vibro-acoustic analyses is much simpler than the actual car model which is normally used by Ford Otosan. Their models include millions of degree of freedom which can not be handled by the computers that we have at Koç University. The simple model with nearly 30.000 degree of freedom was also generated at Ford Otosan to represent the actual model especially at the frequency range that is considered. The simple model includes only the external bulk model of the car cabin and the application points for the force data coming from the engine. As seen from the figure 2.4, there aren't any components between the body and the engine force application points.

To make the model simple, these application locations were connected to the vehicle body rigidly. Because of all these simplifications, the simple structural model is expected to have slightly different simulation results compared to the detailed Ford model. The difference can be seen clearly in the following figure 2.3

2.2 Finite Element Model

Figure 2.4 shows the structural model used for uncoupled analysis.
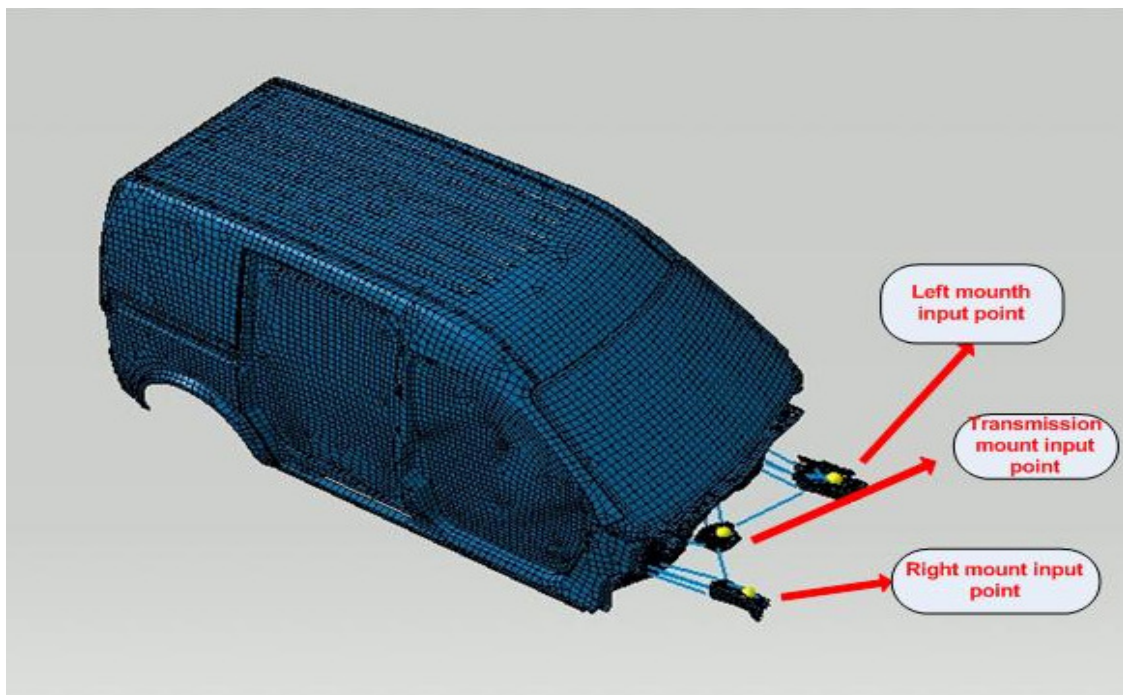
Figure 2.4: Structural Finite Element Model showing the engine mounts as the disturbance input locations

In this model, SHELL181 and MASS21 were used as element types. After determining the element types and identifying material properties, modal analysis was performed in the frequency range of 0-160 Hz. The analysis model only includes the hull system enclosing the cavities of the vehicle and the engine mounts are simply connected to the main body by welding. The main structure of the vehicle was modeled by using shell elements with different thicknesses. MASS 21 element type was used to represent the welding of the engine mounts to the main structure. The properties of the SHELL and MASS element is stated in the Table 2.1

Young modulus	2.1e+014 N/m^2	2.1e+014 N/m^2
Poisssons Ratio	0,30	0,30
Density	7.85e+006 kg/m^3	7.85e+006 kg/m^3

Table 2.1: Material properties of the structural Model

The forced response analysis for obtaining the velocity boundary conditions required for the uncoupled analysis was performed in the same frequency range (0-160 Hz) with an interval of 1 Hz. The force disturbances, measured experimentally at the engine mounts, were used as the disturbance source for the structure. A global 1% structural damping was introduced. From the analysis, the velocities were obtained at every finite element node and then used as velocity boundary conditions in the uncoupled vibro-acoustic analysis.

2.3. The Cavity (Acoustic) Finite Element Model

In order to analyze interior noise, the acoustic cavity of the vehicle needs to be both defined and meshed. As for any FE analysis it is important to create an accurate, realistic model. In order to analyze the interior noise, the interior (volume) should be meshed such that the vibration from the structure can be transferred to the cavity across the outer envelope of the cavity mesh.

Cavity mesh (volume mesh) was created directly from the structural finite element model in LMS Virtual Lab (SYSNOISE). The same cavity geometry seen below in the figure 2.5, which includes a mid-panel separating the cavity into two divisions, was used in all vibro-acoustic analyses including coupled and uncoupled analysis.
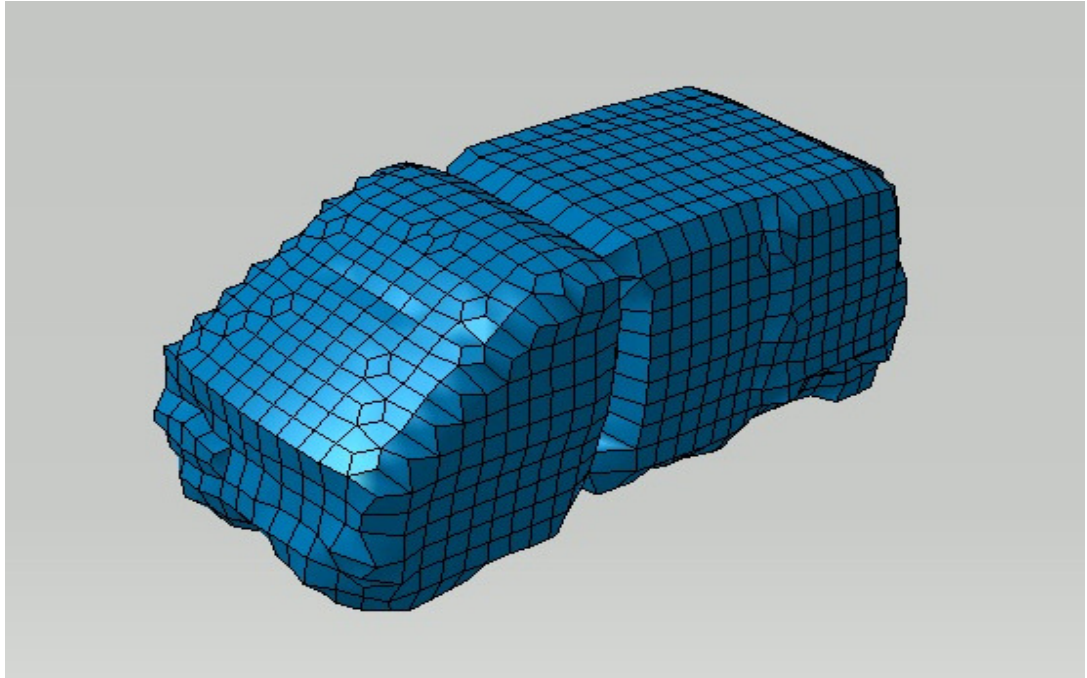
Figure 2.5: Cavity Finite Element Model

At first, the holes in the geometry are detected and repaired to define a cavity. The meshing algorithm mostly uses HEXA element type. In case of any disagreement between the structural and cavity mesh, it may add PENTA element type. That's why it is easy to handle sharp and smooth features.

2.4 Mesh mapping

As seen from figure 2.4 and figure 2.5, the structural and cavity meshes are quite incompatible. Therefore, a mesh mapping is required to link these incompatible meshes.

The method used in Virtual Lab starts by creating automatically the envelope of the main cavity. Then, it is introduced to the software that every node on the envelope should be linked to the intended nodes on the structural mesh. Then, a distance value "Y" and a maximum number of nodes "X" on the structural mesh are defined, which means the software will generate a mesh mapping matrix on one node of the envelop mesh to maximum X nodes on the structural mesh within a distance of Y mm. The nodes of the structural mesh that are linked to an acoustic node are called the wetted surface nodes. For the analyses in this thesis, distance was assigned as 50mm and the maximum node number was 4. This is normally sufficient to have a good coupling between the structural and acoustic mesh.

2.5 Engine Disturbances Model

Engine forces are considered to be transferred to the structure at the mount application points. As it can be seen in the figure 2.4, there are three engine mount locations which are called left, right and transmission engine mounts. Each of them has three directions (x, y, z) where the amplitudes may vary (see figure 2.6). Figure 2.6 shows the amplitude variation of the force data that is measured experimentally at the mount locations while the engine is running at different engine speeds. The study will be focusing on the causes of the mid-speed boom that occurs around 2500-3000 rpm. This rpm range corresponds to 93-100 Hz, because the engine is four-stroke engine, and on four-stroke engines, each cylinder is fired

once for every two revolutions of the crankshaft, which means we should focus on 2nd harmonic force data.
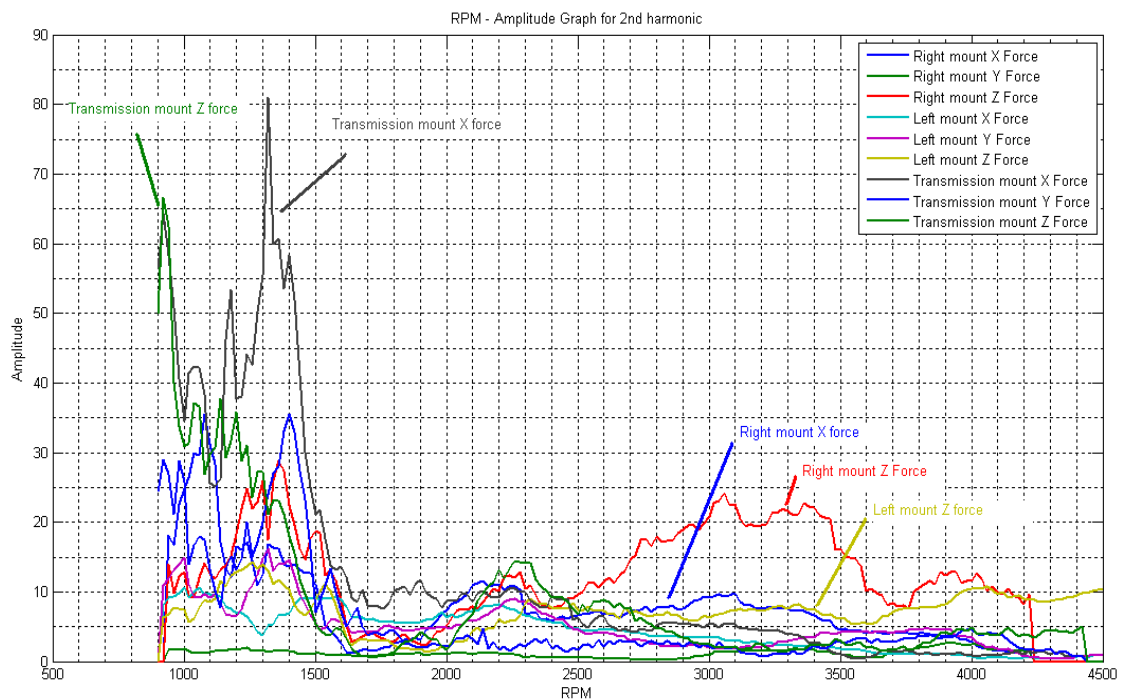
Figure 2.6: The amplitudes of engine forces

2.6 The Uncoupled Analysis Process Steps

In the vibro-acoustic analyses, the software LMS Virtual Lab is used. The steps followed in the uncoupled analysis is shown in Figure 2.7
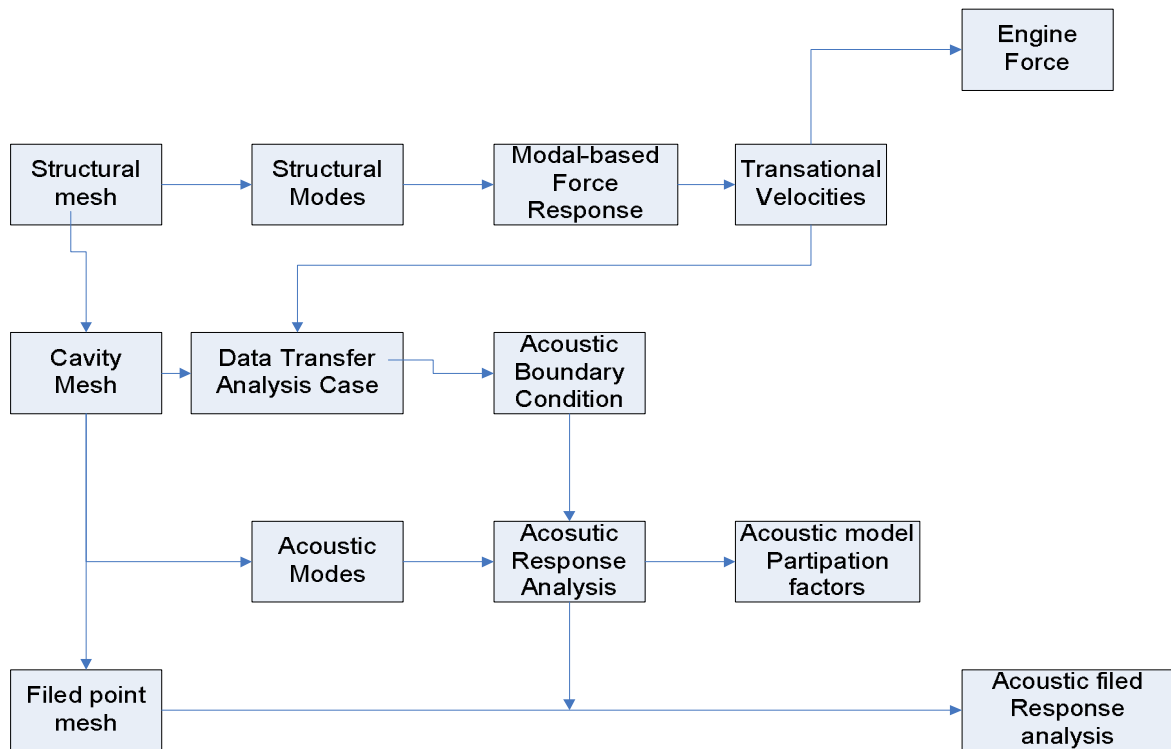
Figure 2.7: The Uncoupled Analysis Process Flow

Structural mode shapes and natural frequencies were calculated in NASTRAN. In

NASTRAN using Lanczos Method (SOL 103) the natural frequencies and the mode shapes

of the structure is calculated between 0-200Hz frequency range.

Then the result file, which includes the finite element geometry and mode shapes

and natural frequencies, was imported to SYSNOISE and the engine forces were assigned

to related mount locations. After assigning magnitudes and directions of force data to the related application points, a harmonic analysis called "Modal Based Force Response Analysis" was performed in SYSNOISE and as a result translational velocities of all nodes on the structural mesh were obtained.

After completing the structural analysis, some preparations should be done before the acoustic analysis. At first, cavity finite element model, seen in figure 2.5, was created from structural finite element model in LMS Virtual Lab. Then a field point mesh (figure 2.8) representing the head of driver was created. As a final step before performing the acoustic analysis, boundary conditions should be designated for the cavity model. The translational velocities of each node on the structural mesh, which were obtained at the end of Modal-Based Force Response Analysis, were introduced as the boundary conditions for the acoustic domain.

After completing preparation steps, the acoustic analysis called "Acoustic Response Analysis Case" was performed. After that, sound pressure levels can be visualized for all locations in the cavity. As a last step, Acoustic field Acoustic Response Analysis was performed and sound pressure levels were obtained on the field mesh (figure 2.5), in other words at the location of the driver's head. However the result of the acoustic response

analysis case is pressure vectors therefore a process called " vector to function conversion

case" is applied to convert the pressure vectors to scalar dB(A weighted) values.
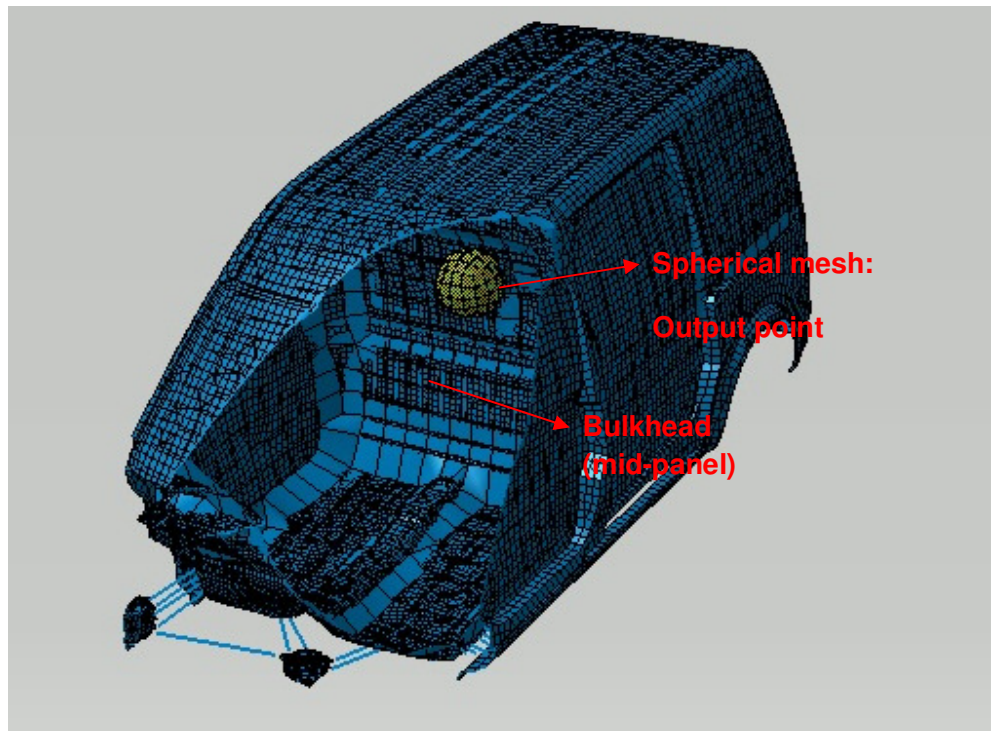
Figure 2.8: Spherical field mesh that represents the driver head, where the output points are placed for the SPL values.

2.8 ATV based technology

Since every acoustic system can be considered as a linear system, we can establish a linear input-output relationship between the "input" of an acoustic system, mechanical surface vibrations that generate sound waves, and the "output" of an acoustic system, the sound pressure at a number of locations in space. If we subdivide the vibrating surfaces into a finite number of discrete "patches" or vibration panels, we can express this relationship in the form of the following matrix equation [5]:

{Sound Pressure} = [Acoustic Transfer Matrix] x {Surface Velocities}

where *{Sound Pressure}* is a column vector containing the sound pressures at the different locations, {Surface Velocities} is a column vector containing the structural velocities of the vibra*t*ing panels and [Acoustic Transfer Matrix] is the system matrix relating input and outputs.

The surface velocities of the vibrating panels are the normal component of the structural velocities, since only this normal component plays a role in the generation of sound waves.

Representing the surface velocities column vector by $\{v_{ns}(\omega)\}$ (the index "ns" referring to normal structural velocities) and consider the sound pressure level p at a single

microphone location, we can hence write (where w highlights the frequency dependence of the relation):

$$p = \{ATV(\omega)\}^T . \{v_{ns}(\omega)\}$$

(2-1)

Therefore, the Acoustic Transfer Vector concept (ATV) is an ensemble of Acoustic Transfer Functions relating the normal vibration velocities of a number of discrete panels to the sound pressure at a single microphone location

By definition, an Acoustic Transfer Vector is completely determined by the characteristics of the acoustic system under consideration and therefore only depends on the following system parameters such as geometry of the vibrating surfaces, acoustic treatment of the surfaces, i.e. absorption linings represented by impedance or admittance boundary conditions, frequency, physical properties of the acoustic medium (speed of sound & density)

As shown by the equations, the acoustic response is found simply as the matrix product of the ATVs with the operational structural response, which allows the same set of ATVs to be re-used to compute and compare acoustic performance for many different situations:

- Effect of structural modifications without changes to the actual surface geometry (e.g. adding internal stiffener ribs)

- Performance for different sets of operational conditions, e.g. corresponding to different RPMs for a petrol or diesel engine or a reciprocating compressor

It is clear that the use of ATVs will result in huge savings in computation time when acoustic performance for many different operational structural responses has to be evaluated.

The Acoustic Transfer Vectors from the radiating surface to specified field points are evaluated in the first step across the frequency range of interest at fixed frequency intervals. In the second step, the acoustic response in the field points is calculated for all loading conditions by combining the ATV with the normal structural velocity boundary condition vector at any frequency within the range. In this thesis 0-200Hz frequency range is used in the ATV Analysis.

One of the important advantage of this technique is that the frequency dependent ATV's can also be used for contribution analysis, by a 'partial' vector-vector product only taking into account the normal velocity boundary conditions on part of the radiating surface,

$$p_c(\omega) = \{ATV(\omega)^e\}^T\}.\{v_n(\omega)^e\} \qquad (2\text{-}2)$$

where the superscript e denotes an element contribution. This way, the contribution of groups of elements, corresponding to distinct panels of the structure, can be derived.

2.9 The Steps of Panel Acoustic Contribution Analysis (PACA)

As presented in the previous chapters, for the acoustic investigation and the main concern of this study; for the optimization; Panel Acoustic Contribution Analysis is used. Like the analysis that we described as the vibro-acoustic Analysis, PACA Analysis is similar, it both uses the FE/BE Approach and ATV technology as well. Only difference is instead of obtaining the SPL values from the driver head, we could also determine the contribution of each panel to the SPL as well.

The steps of the Panel Acoustic Contribution are presented in the Figure 2.9.
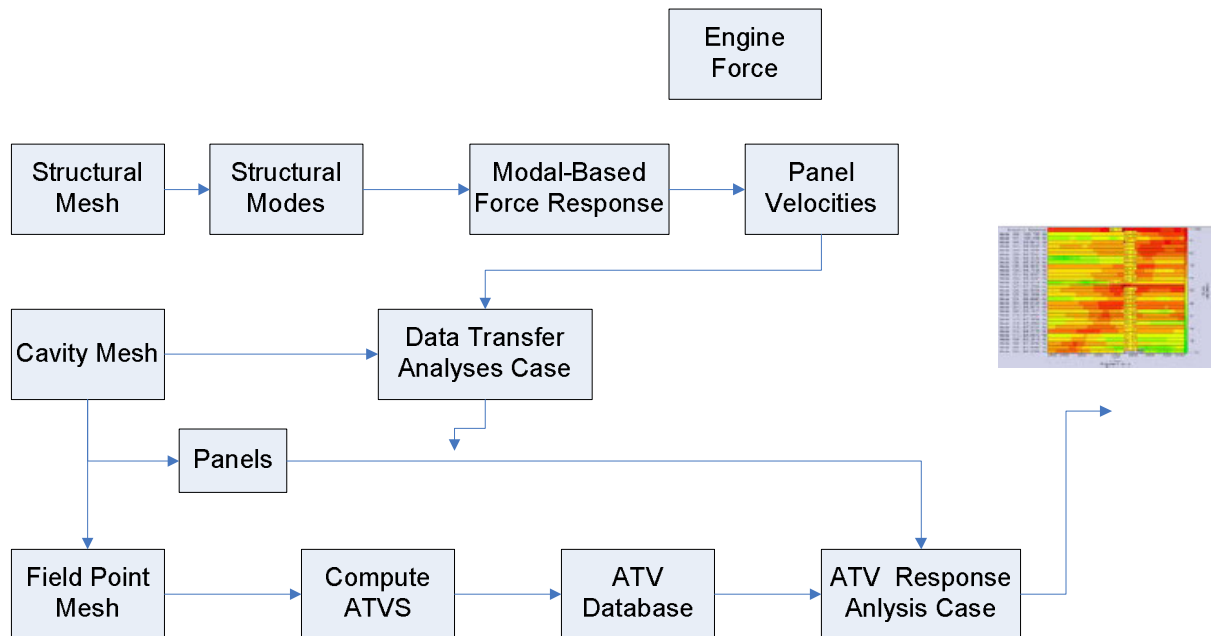
Figure 2.9: Panel Acoustic Analysis (PACA) Process Flow Diagram

Like the other analyses, there are many similarities with the steps of the previous analysis. The structural analysis is same in the PACA analysis. For instance, at first the structural modes are calculated in Nastran and the harmonic Analysis which is called Modal Based Force Response Analysis is performed. The panel normal velocities are obtained as the result of the Modal Based Force Response. Like the other analysis, cavity

mesh is created like in the coupled and uncoupled analysis using the advanced cavity mesher module in LMS Virtual Lab.

In our vehicle model, for the PACA Analysis panels are created on the vehicle model to investigate the contribution of each panel. The colorful image of the created panels figure is presented in Figure. 2.10
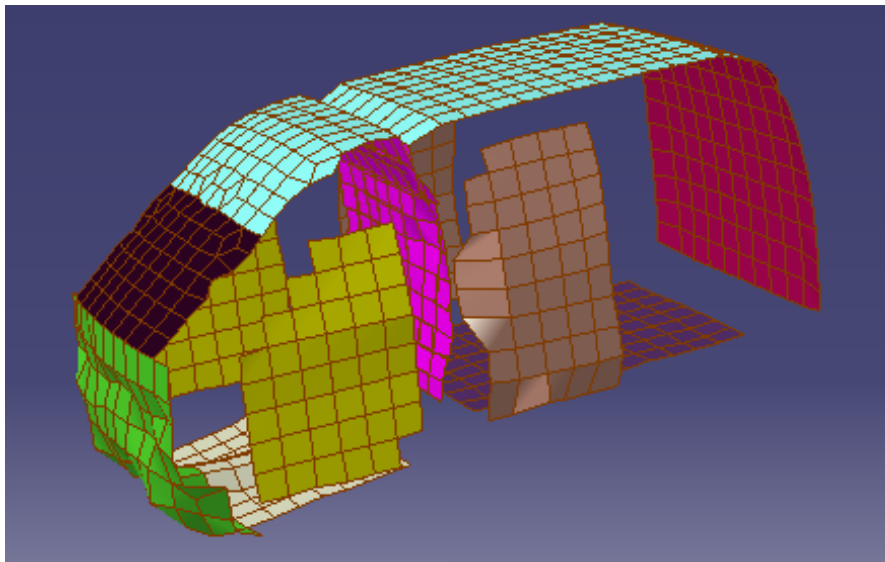
Figure 2.10: Panels created on the cavity model

In the PACA Analysis   8 panels are created and their contributions to the sound pressure levels are gathered. The table that shows the panels and corresponding color of each panel is presented in Table 2.1

COLOR	PANEL NAME
Green	Front panel
Blue	Roof
Yellow	Front doors
White	Front floor
Pink	Bulkhead
Dark blue	Back floor
Red	Back panel
Dark brown	Window

Table 2.2: The panels used in PACA Analysis and on the left side the corresponding color that resembles the related panel.

Similar to the uncoupled analyses, the module of data transfer was implemented to transfer the velocities. The field point mesh symbolizing the head of the driver is created and the acoustic transfer Vectors.(ATV's).The data transfer analysis results and ATVs are imported within the analysis and ATV response analysis is performed and the contribution of each panel is obtained.   The nominal result of PACA Analysis, showing the panel contribution and the SPL values are presented figure 2.11 and 2.12
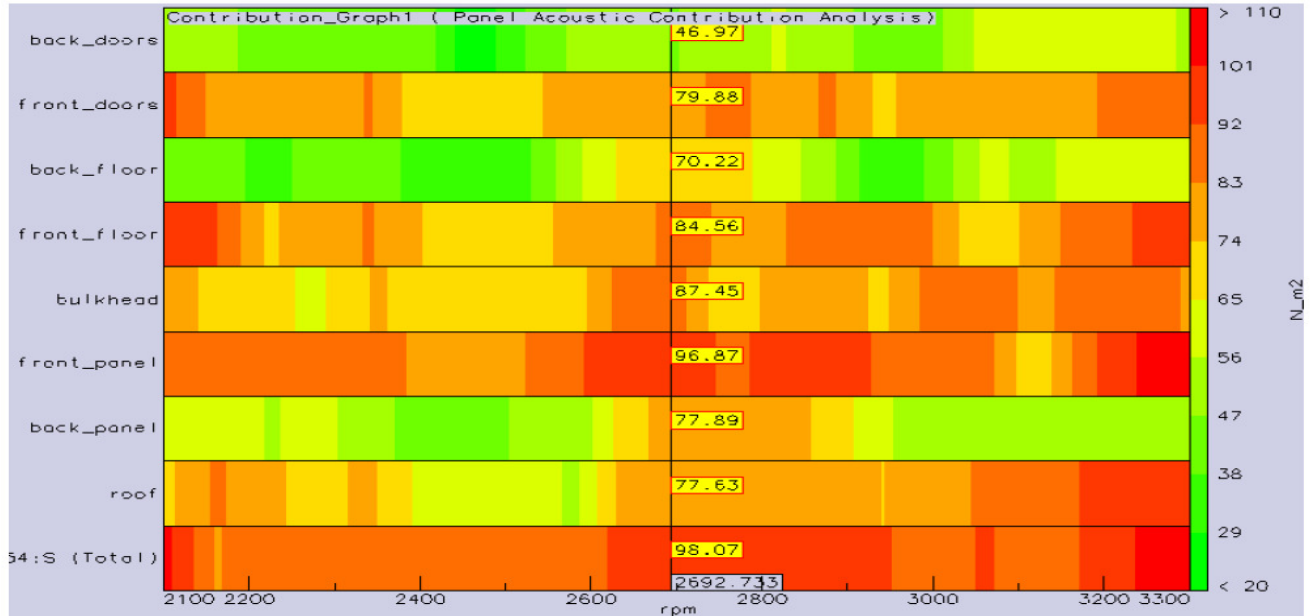
Figure 2.11: Panel Acoustic Contribution Analysis result plot

Figure 2.8 shows the results of PACA Analysis. The x-axis shows the engine speed in RPMs. The y-axis is divided into segments to show the contribution of each panel. Red colored parts represent high contribution, in the order of more than 90 dB(A)s, and yellow colored parts represent low contribution, less than 60 dB(A)s, to the overall sound pressure level. According to PACA results, all panels except back floor and doors have contribution at different engine speeds, changing from 900 to 4500 RPM.

Therefore with the insight of this PACA Analysis we could define our design parameters and find the optimum configurations according to a specified objective which will be discussed in Chapter 4.
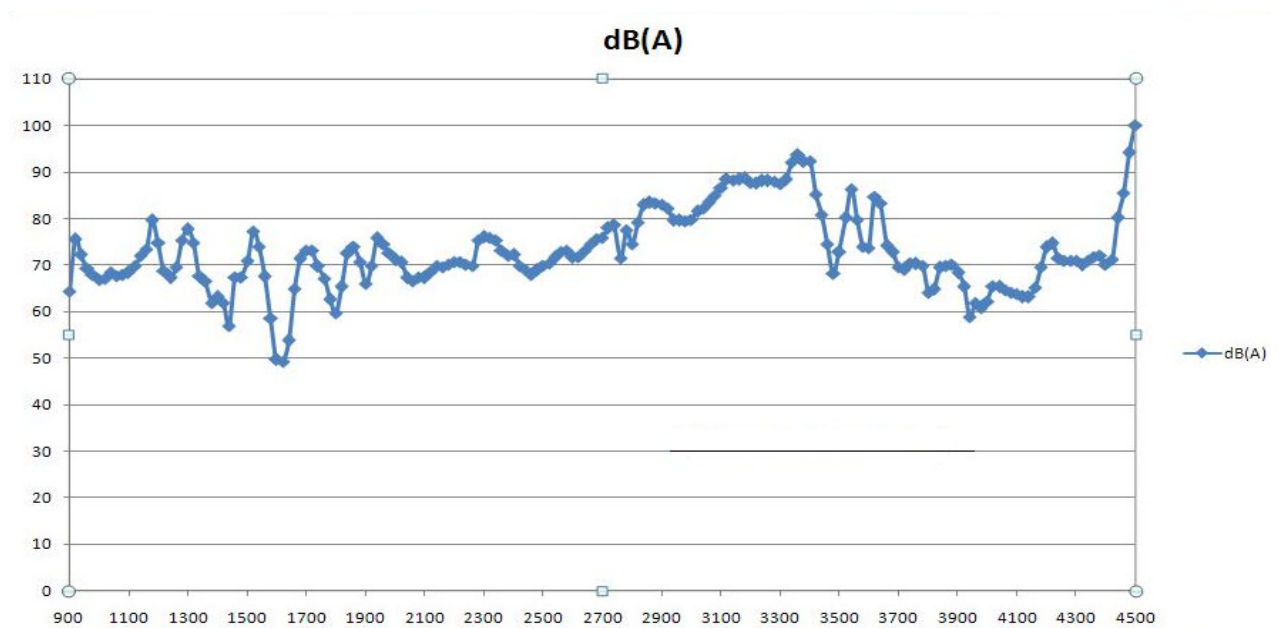
Figure 2.12: Sound Pressure Values in dB(A) obtained from the driver's head

Figure 2.9 shows the pressure values in dB(A) obtained from the drivers head in the same PACA analysis as well. X axis represents the pressure values whereas Y values represent the rpm values. The pressure values between 2800-3700 rpm have more influence on the

overall SPL therefore for the rest of the optimization vibro-acoustic analysis rpm range is limited to the 2800-3700rpm.

By performing the Panel Acoustic Contribution Analysis (PACA), the contribution of each radiating panel to the interior noise is calculated. With the help of the PACA the user can identify the most critical radiating panels. Then this information could be used in the optimization process to reduce the cabin noise by giving importance to these critical panels. The results of the PACA includes a lot of information however the PACA results are only based on the nominal design therefore the PACA analysis results do not sustain any information such as how these panels should be modified so that the sound pressure levels can be reduced. .According to the PACA analysis the most contributing panels are; ***back floor, front floor, front doors, bulkhead, window, front panel , roof .*** In our optimization analyses, the thickness of these 7 panels will be our design parameters.

Chapter 3
Theory
Design of Experiments & Response Surface Modeling and Optimization

3.1 Overview

In chapter 2 the vibro-acoustic analysis was performed and the most contributing panels to the interior noise were identified. These panel thicknesses will be used as design variables for the Design of Experiments (DOE) studies. Response Surface Models will be built using the results of DOE studies and optimization studies will be performed on these models to obtain the optimum panel configurations to improve the sound pressure levels inside the passenger cabin. The DOE, RSM and optimization algorithm details are described in the following sections.

3.2 Background on DOE & RSM

DOE is a statistical methodology that is primarily concerned with the development of an effective experimentation plan. The fundamental ideas of DOE were introduced by R.A. Fisher in the 1920s to address agricultural experimentation problems [20]. DOE methods have since evolved into a comprehensive body of theory and application tools, and are being widely used in natural sciences, industrial, and engineering applications due to their

effectiveness [21]. Fundamentally, DOE aims to determine the appropriate set of experiments that are sufficient to attain the desired level of information by varying the main factors of interest over an operating range in a structured manner using statistical tools.

The fundamental goal of RSM is to obtain an approximate functional relationship between the input variable(s) and the output objective function(s) to construct a model over the entire domain of interest. A common method to obtain this model is to employ regression, which relates controllable variables to responses. The regression equations provide information about the properties of the system from which the data (generally obtained through a set of designed experiments) is taken, and can be used to improve/optimize processes through appropriate deterministic optimization procedures. Myers et al., [22] review the progress of RSM in the general areas of experimental design and analysis, and indicate how advances in other fields of applied sciences have affected its role. For further references on RSM methodology and applications, the reader is referred to [23]. The increased use and availability of computational models to assess performance of different product designs has allowed the use of RSM for computer experiments (rather than physical experiments for which RSM has been initially developed). The use of RSM presents two fundamental advantages over other optimization schemes (e.g., random search schemes such as genetic algorithms). First, RSM yields a functional relationship between the factors (i.e., various components and parameters of the product design) and response

variables (i.e., some performance metric for the design) of interest over the search space. This provides a better understanding of the system behavior, and complements the product designer's expertise with the system. The step-by-step nature of the technique also allows interaction of the designer with the optimization scheme. Secondly, such functional relationships (obtained through regression analysis, in general) allows for much faster search of the design space compared to random search schemes. This is particularly important for computer models that require significant amount of computational time to run.

In the domain of acoustic analysis, the following studies are noteworthy, and are relevant to our work. Liang et al. [24] utilized DOE (in particular a three-level fractional factorial design) to optimize three response variables with respect to three factors (two thicknesses and one material). The authors obtained (through regression analysis) a response surface to analyze the effect of design parameters on the sound radiation from a vibrating panel with point force excitation. The authors approximated the structure-born noise problem by a series of second-degree polynomials, and considered three objectives of mean quadratic velocity, sound radiation power and system loss factor. The paper presents a simple case study to demonstrate the effectiveness of the methodology. The study presented in [25] is similar; the authors used Central Composite Design (instead of a three-level fractional factorial design) in this paper. In an earlier study by Kamci et al. [26], a screening study was performed for the thicknesses of seven panels surrounding the cabin to identify the panels

that have the highest contribution to sound pressure level. Fractional factorial design was selected for the DOE analysis and the most significant panels were determined. Marburg and his co-workers [12], [13], [14] and [15]published series of papers on the investigation of vibro-acoustic interior noise of the vehicles and the optimization of several structure-acoustic systems.

3.3. Two Level Full Factorial Experimentation

In this thesis, we employed techniques from the fields of DOE to understand the relationship between the studied design parameters and sound pressure level. The PACA results were chosen as the basis for the DOE study. A Two Level Full Factorial Experimentation was employed to find the significant design parameters. Two level full factorial experimentation is a common experimental design with all input factors set at two levels each. These levels are called `high' and `low' or `+1' and `-1', respectively. A design with all possible high/low combinations of all the input factors is called a two-level full factorial design. The number of the experiments of a two level-full factorial design is 2^k where k is the number of factors [20].

In order to determine the panel thicknesses that are the highest contributors to the structure-borne interior noise, a study was performed using DOE. For this purpose, the first seven factors listed in Table 3.1 (Factors A to G, excluding Factor H) were considered. Back door thickness (i.e., Factor H) was not taken into account due to the fact that sound pressure

level is measured in the passenger cabin only, and back doors are known to contribute minimally to the total sound pressure level. For each factor, two-levels of settings were used (a high level and a low level). For example, front panel thickness (Factor F) was set at two levels of 0.72 mm (low level) and 0.88 mm (high level). The high and low levels for each factor were determined by increasing and decreasing the baseline values of the factors by 10%, respectively.

A full-factorial experiment was employed which required 2^7 (=128) runs. An additional run was added to test the factors at their baseline values (e.g., Factor F was set to 0.8 mm for this run), which was also used to check for curvature in the RSM analysis.

Table 3.1: Panel thicknesses considered in DOE study (low & high values are also included)

Factors	Panel Name	Baseline Thickness (mm)	Low (mm)	High (mm)
A	Back floor	0.9	0.81	0.99
B	Front floor	0.8	0.72	0.88
C	Front & Back doors	1.0	0.90	1.10
D	Bulkhead	0.8	0.72	0.88
E	Window	5.0	4.5	5.5
F	Front panel	0.8	0.72	0.88
G	Roof	0.7	0.63	0.77

Four Response Variables are selected in DOE study as our performance metrics (objective functions). The vibro-acoustic analysis were employed 129 times (number of experiments required for the full factorial design) for each metric and the results were used for the regression analysis to obtain the response surface. The explanation of each metric is as follows:

"Percentage over 80dBA" Metric

The response variable was selected as the fraction of RPMs that are greater 80 dB(A) within the engine speed range of 2800 to 3700 RPMs (this range corresponds to 46 distinct engine speeds due to 20 RPM increment used in evaluating sound pressure level for a given engine speed). This metric is preferred when more than one SPL values are over the threshold value. In this study, 80 dB(A) is selected as the threshold but this value can be altered based on the desired noise levels defined by the automobile manufacturers. After the DOE is completed, there are 129 experiments including the centroid point (the configuration with the baseline values of the design variables). The percentage values of the full-factorial experiment vary between 17.39%-69.56%. The percentage value obtained for the baseline configuration is 67.39% and with the minimization of the objective function, it is expected that this value will be improved.

"Max Amplitude" Metric

In some cases, the highest amplitude of SPL can be the focus of the redesign efforts. In those cases, there is only one dominant peak that stands out in the SPL performance and the rest of the SPL values are in the acceptable range. In this metric, the response variable was selected as the max SPL amplitude (dBA) within the engine speed range of 2800 to 3700 RPMs. The max amplitude values of the full-factorial experiment vary between 89.73-118.42 dBA. The max amplitude obtained for the baseline configuration is 93.97 dBA and it is expected that with the minimization of the objective function, this value will be improved.

"RMS Performance" Metric

In some cases, overall amplitude of SPL values can be in consideration in the redesign studies. In this metric, the response variable was selected as the root mean square (rms) of the SPL values within the engine speed range of 2800-3700 RPMs. The rms values of the full-factorial experiment vary between 71.79 -88.52 dBA. The RMS value obtained for the baseline configuration is 86.51 dBA and it is expected that with the minimization of the obejective function, this value will be enhanced.

"Idealized Performance Error" Metric

Usually, automobile manufactures have a desired performance curve for the SPL as the engine speed increases. This curve is usually an idealistic curve and usually hard to achieve. However, the NVH designers would like to approach this curve as much as possible. A linear relationship between the SPL and the engine speed was defined as the desired performance curve. In this metric, the response variable was selected as the least mean square error (mse) between the idealized curve and the SPL predictions for a given design. The mse values of the full-factorial experiment vary between 62.69-419.45 dBA. The mse for the baseline configuration is 173.12 dBA and it is expected that with the minimization of the objective function, this value will be improved.

3.4 Response Surface Modeling

A response surface is a hyper-surface which describes the relationship between the experimental factors (inputs) and the values of one or more measurable responses (outputs). Once a DOE is performed, usually a response surface model will be generated to fit the experimental results to get a better insight in the design problem.

In general all *RSM* problems use either one or the mixture of the both the first-order and second order models. In each model, the levels of each factor are independent of the

levels of other factors. In order to get the most efficient result in the approximation of polynomials the proper experimental design must be used to collect data. Once the data are collected, the ***Method of Least Square*** is used to estimate the parameters in the polynomials. The response surface model is usually assumed as a second-order polynomial, which can be written for n_v design variables below [20]

$$y^{(p)} = c_o + \sum_i c_i x_i + \sum_{1 \le i \le j \le n_v} c_{ij} x_i x_j \quad p = 1, \cdots, n_s \tag{3.1}$$

Where $y^{(p)}$ is the dependent variable of the response surface model, c_o, c_i, c_{ij} are the regression coefficients, x_i is the design variable, and n_s is the number of observations. The basis functions for the regression model of Equation 3 lead to an over-determined matrix problem and the regression coefficients are obtained to minimize the total statistical error.

3.5 Numerical Optimization

Simulation is a powerful tool in science and engineering for predicting the behavior of physical systems. Using today's simulation tools it has now become practical to consider complex design problems, where people wish to determine parameters of large systems that

maximize a certain objective. These types of problems are naturally posed as optimization problems. This simulation-based optimization process adjusts the input variables of simulation model to find the levels that achieve the best possible outcome [27]

Due to the number of objective functions, numerical optimization can be classified into subfields; *Single-objective optimization* contains one single objective that needs to be optimized. We could classify our analysis as single-objective optimization since we had only one optimization output parameters in all our studies. However Multi-*objective optimization* has multiple objectives to be optimized which sometimes require more complex algorithms for finding the optimum configurations.

3.5.1 Global optimization method

Global Optimization is the method that we used in our optimization analysis. Global optimization is the task of finding the absolutely best set of input variables to optimize an objective function. There are several types of global optimization methods, deterministic methods (e.g., branch and bound method), stochastic methods (e.g., direct Monte-Carlo sampling) and most popular the heuristics methods (e.g., Evolutionary algorithms, Simulated annealing) . These methods have a good possibility to find the global optimum, but this is not guaranteed [28].

In our analysis we used the *heuristics methods* as the global optimization methods. The heuristics methods are probability-based searching methods, and they search the design space in an more intelligent way. The advantage of these methods is that these methods have a good possibility to find the global optimum, because they search for an optimum based on global information.

3.5.1.1 Differential Evolution

Differential Evolution (DE) is used as the optimization algorithm in the studies. DE is a recent approach for the solution of real-valued multi-dimensional optimization problems [29]. As is typical for stochastic search algorithms, differential evolution does not require the calculation of the sensitivities. It is a population base randomized search algorithm. At any iteration, a set of solutions (population) is kept and updated by adding the weighted difference between a defined number of randomly selected members of the previous population to another member. In all of the optimization studies, the objective functions were minimized and 35*50 iterations were performed to find the optimum set of solutions. The optimum solutions for the three metrics are given in Table 4.2.

CHAPTER 4

Results of Design of Experiments, Response Surface Modeling and Optimization Studies

In this part, the computer based optimization of the commercial vehicle model is described. The steps of the optimization process and also the theory underlying the optimization are introduced throughout this part.

Throughout this thesis, the theory and the steps of the vibro-acoustic analysis process was presented. In this study, since the main concern is to reduce the interior sound pressure level, an optimization process which uses the design of experiment methodology upon the vibro-acoustic analysis is performed.

In this study, we employ techniques from the fields of Design of Experiments (DOE) to understand the relationship between the studied design parameters and sound pressure level. The PACA results are chosen as the basis for the DOE study. The thicknesses of the same panels used in the PACA are used in a DOE study to identify the important ones. Following the DOE analysis, response surfaces are built to be used for the optimization studies. Preliminary optimization studies are employed using the regression models generated in the Response Surface Modeling (RSM) study. (See Appendix 1 for the DOE analysis results and example response Surface Models for the optimization studies).

4.1. Optimization Process Flowchart

Although the results of the PACA contains a lot of useful information, it does not provide any guidance to the designer regarding how these panels should be modified so that the sound pressure levels can be reduced. The PACA results are only based on the current design and they do not provide any information regarding how the performance changes if any or all of these panel design variables are changed within a certain range. The vehicle contains many structural panels and consequently, there are many design variables that should be looked at when a redesign effort is considered. Especially, when the coupling between the structure and cavity and the interactions between the panels are considered, the reduction of sound pressure level forms a highly non-linear optimization problem, and hence is still considered to be a complicated task even for a simple vibro-acoustic problem.

We complement the results of PACA by employing a DOE study to determine the impact of various panel thicknesses on the sound pressure level. Figure 4.1 shows the process flow for the optimization study performed in this thesis. Observing from PACA results that front floor, front door, bulkhead, window, front panel and roof panels were all significant contributors to the sound pressure level, we decided to choose the thicknesses of these panels as our design factors. We narrowed our study to the engine speed range of

2800 to 3700 RPM, since the highest values of sound pressure level occur in this range of

RPMs
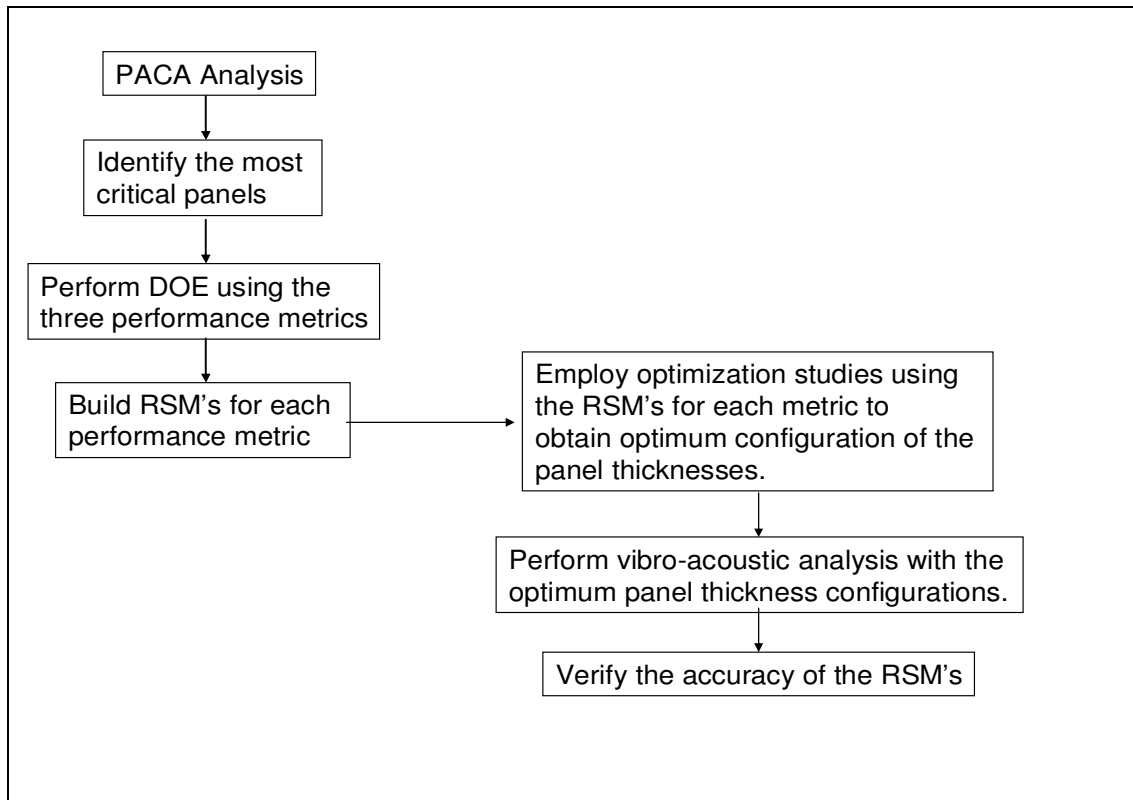
Figure 4.1: Optimization process flow chart.

The results presented with the bar charts in Figures 4.2, 4.3, 4.4 and 4.5 shows the

contribution of each design variable to the performance metric under consideration. When

the results of the four metrics are compared, it is observed that among the seven panels

considered, front panel is the most significant for all of the metrics considered. The front

doors are also significant for the "Max Peak" and "Idealized Performance Error" metrics.

The two way interactions of the panel thicknesses are also taken into account in the

regression model. Interesting observations can be made from the contribution plot. There are cases when the significance of a single design parameter in the overall response may increase when the two way interactions of factors are considered (eg. "Max Amplitude metric": roof only contribution vs roof and front panel thicknesses interaction contribution).

When the regression parameters are considered, the adjusted R^2 of the "Percentage over 80dBA" metric is 0.977. That means 97.7 % of the variability in the response variable can be explained with the regression model. The adjusted R^2 of the "Max Peak", "Idealized Performance Error" and "RMS" metrics are 0.773, 0.983 and 0.704 respectively. Based on these adjusted R^2 values, the regression models are acceptable and they can be utilized for the optimization studies
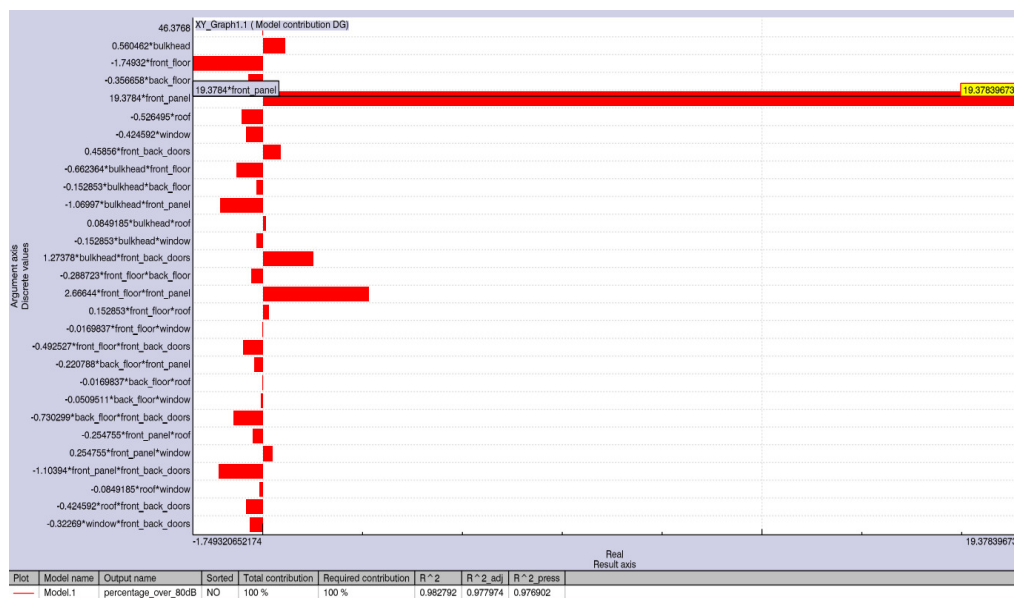
Figure 4.2: Contribution chart of the design variables for the "*Percentage over 80 dBA*" metric
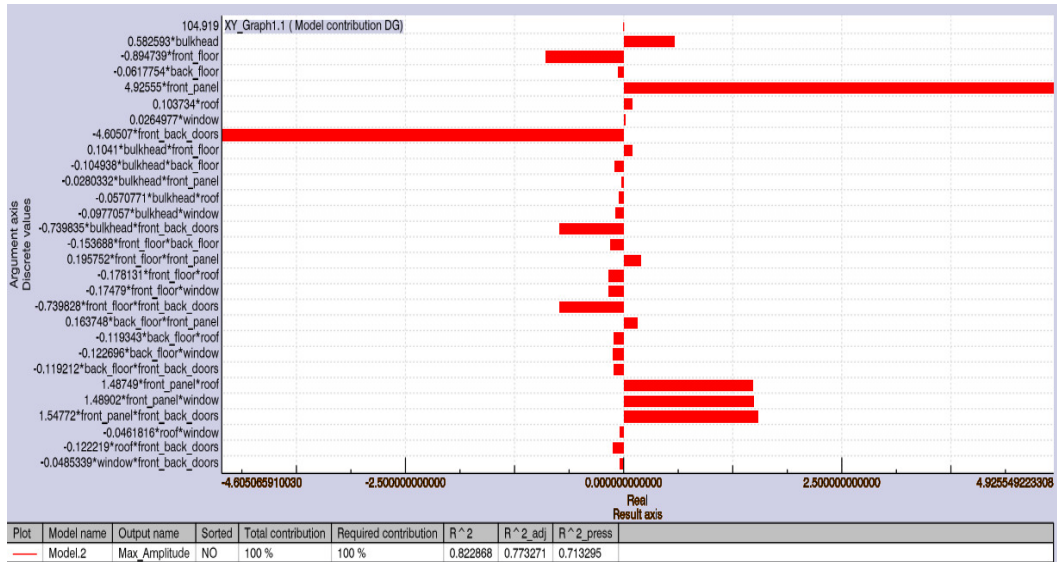
Figure 4.3: Contribution chart of the design variables for the "*Max Amplitude*" metric
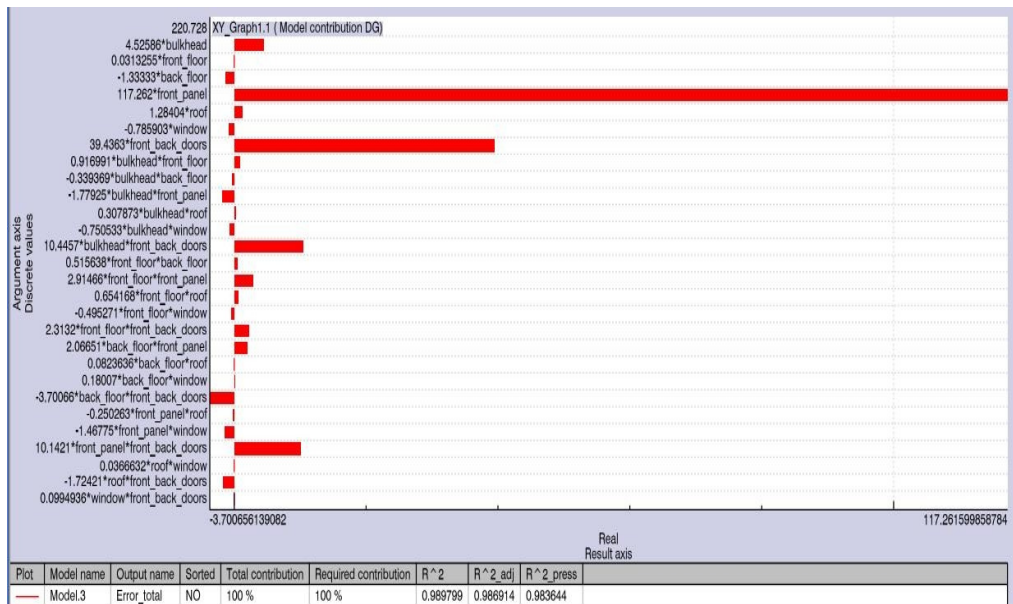
Figure 4.4: Contribution chart of the design variables for the "*Idealized Performance Error*" metric.
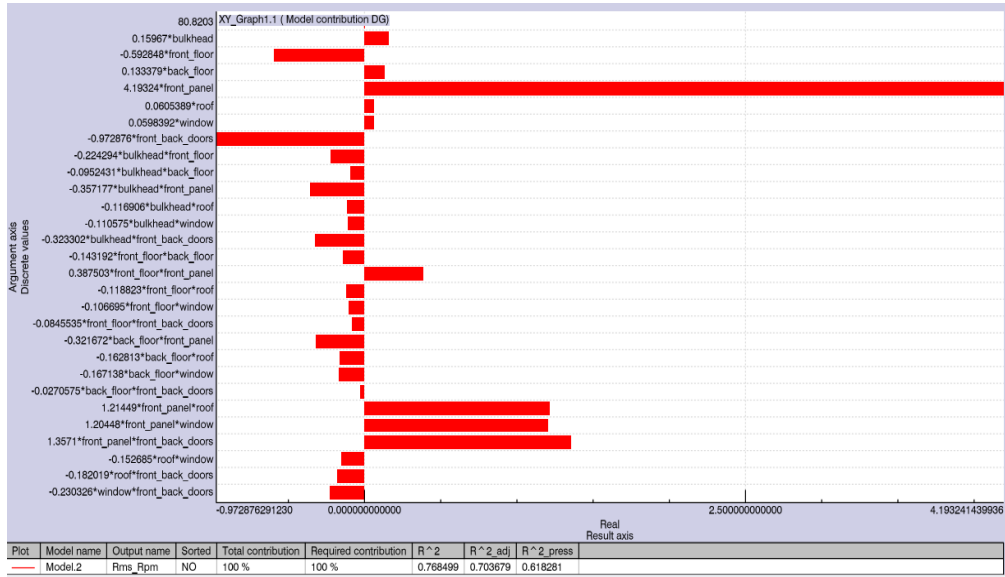
Figure 4.5: Contribution chart of the design variables for the "*RMS*" metric

4.2 Optimization Results

After the RSM analysis, optimization is performed using the regression models obtained based on the three performance metrics. There are same parameters that have to be set in the LMS optimization tool for differential algorithm. These parameters are;

— Population Size

— Initial stepwidth

— Weighting factor

— Inverse crossover probability

— Average stopping stepwidth

— Maximum number of iterations

Population Size: The population size defines the number of designs that are evaluated during each iteration (generation). The number must be >7, otherwise the algorithm gets trapped in an endless loop. The population size depends on the number of design variables (parameters): a good choice is more than 5 times the number of variables. ***Since we have 7 parameters in our analyses we used a population size of 35***.

Weighting factor could be between 0.5 and 1. A weighting factor close to the 1 increase the optimization accuracy whereas increase the calculation time. Therefore a value between 0.5 and 1 is proffered***. In our analyses we choose a weighting factor of 0.7***

The maximum number of iterations is: nf = number of iterations * population size. If this number is set very low, the optimization might not have found an optimum when stopped. If it is chosen too high, the optimization will stop with the step width stop criterion. Less than 10 iterations are not recommended. In our analyses 30 iterations therefore total 1035 iterations are held in optimization.

The advantage of having a response surface is that the vibro-acoustic analysis and the resulting design variable will not be recalculated when the iterations are performed during the optimization procedure. Only the prediction surface will be used to calculate the performance to evaluate the design variables for various iterations.

Differential Evolution (DE) is used as the optimization algorithm in the studies. DE is a recent approach for the solution of real-valued multi-dimensional optimization problems [28]. As is typical for stochastic search algorithms, differential evolution does not require

the calculation of the sensitivities. It is a population base randomized search algorithm. At any iteration, a set of solutions (population) is kept and updated by adding the weighted difference between a defined number of randomly selected members of the previous population to another member. In all of the optimization studies, the objective functions were minimized and 35*50 iterations were performed to find the optimized set of solutions. The optimized solutions for the three metrics are given in Table 4.1. (See Appendix 2 for the optimization iteration plots)

Table 4.1: Optimized set of solutions for the four Performance Metrics

	Percentage over 80 dBA	Max Peak	Idealized Performance -10%	Idealized Performance -20%	RMS	Nominal Panel
Bulkhead(mm)	0.72	0.87	0.82	0.87	0.87	0.80
Front_floor(mm)	0.88	0.88	0.87	0.87	0.88	0.80
Back_floor(mm)	0.98	0.99	0.87	0.99	0.98	0.90
Front_panel(mm)	0.72	0.72	0.72	0.65	0.72	0.80
Roof(mm)	0.77	0.77	0.64	0.76	0.77	0.70
Window(mm)	5.49	5.49	4.62	5.48	5.49	5.00
Frontdoors (mm)	1.09	1.09	0.91	0.90	1.09	1.00
Optimized result obtained with RSM.	**17.86**	**87.62**	**67.75**	**62.99**	**69.77**	
Optimized result verified with traditional vibro-acoustic analysis.	**17.39**	**90.61**	**68.61**	**62.10**	**71.83**	
Nominal Results	*67.39*	*93.97*	*173.12*	*173.12*	*86.51*	

To validate if the optimized solutions obtained through the Response Surface Model, a vibro-acoustic analysis with the optimized values are also performed and compared with the results obtained through the optimization study. As it can be observed from the Table 4.1, the response variables calculated through the traditional vibro-acoustic analysis match with the values predicted through the response surface model. For the "*Percentage over 80 dBA* "metric, the results are approximately similar (17.8673 with RSM and 17.3913 with standart vibro-acoustic analysis). For the "*Max Amplitude*" metric, the results are slightly different (eg: 87.63 with RSM and 90.61 with standard vibro-acoustic analysis). It is believed that the R^2 value obtained for the "*Max Amplitude*" metric explains 77.3% variability in the response variable so it may affect the accuracy of the predicted response. For the "*RMS*" metric the results are slightly different (e.g 69.77 with RSM and 71.83 with standard vibro-acoustic analysis).). It is believed that the R^2 value obtained for the "*RMS*" metric explains 70.3% variability in the response variable so it may affect the accuracy of the predicted response.

The "Idealized Performance" metric is employed for another set of experiments to investigate the effect of the highest and lowest values selected for the design variables. Considering the fact that the front panel thickness is the most significant contributor to all of the performance metrics, the variation of the front panel thickness is changed to 20%

instead of 10%. The next column in Table 4.1 shows the result of this analysis. As it can be observed from the table, the performance (least mean square error) does not change significantly but the overall effect on the SPL performance will be discussed in the following section.

4.3 Comparison of the Optimized Set of Solutions based on the SPL Performance

Optimization studies with three performance metrics provide three set of optimized panel thickness configurations. These configurations are used and the traditional vibro-acoustic analysis is employed to check if this configuration actually improves the SPL performance as a function of the engine speed. Figure 4.6, compares the baseline configuration result with the optimized configuration results based on the three performance metrics. As it can be observed from the figure, all the optimized configurations perform better than the nominal configuration in general (except the peak around 3350 rpm for the result obtained for the "Percentage over 80 dBA" metric and the "RMS" metric). The results obtained for the "Max Amplitude" and "Idealized Performance" metrics are very close to each other. Also the results obtained for the "RMS" and "Percentage over 80 dBA" metrics are very close to each other. The "desired performance" line shows the required performance of the vehicle set by the manufacturer. It shows that within the allowable range of the design variables, the optimized

configuration does not get better even if we change the metric. The result of the additional study where the range of the front panel thickness is changed to ±20% is shown in Figure 4.7. It is compared with the results of the ±10% variation of the front panel thickness. As it can be observed from the figure, changing the variation range of the front panel thickness makes a difference for the optimized configuration especially between 2950-3200 RPM.

According to the result of the optimized set of panels as can be seen in the Table 4.1, approximately results of the all performance metrics(except some panel thicknesses in Above 80Dba and idealized performance metrics) shows similar tendency in the thickness values as the "optimized" values are gathered which shows the robustness of the solution of the optimization study.
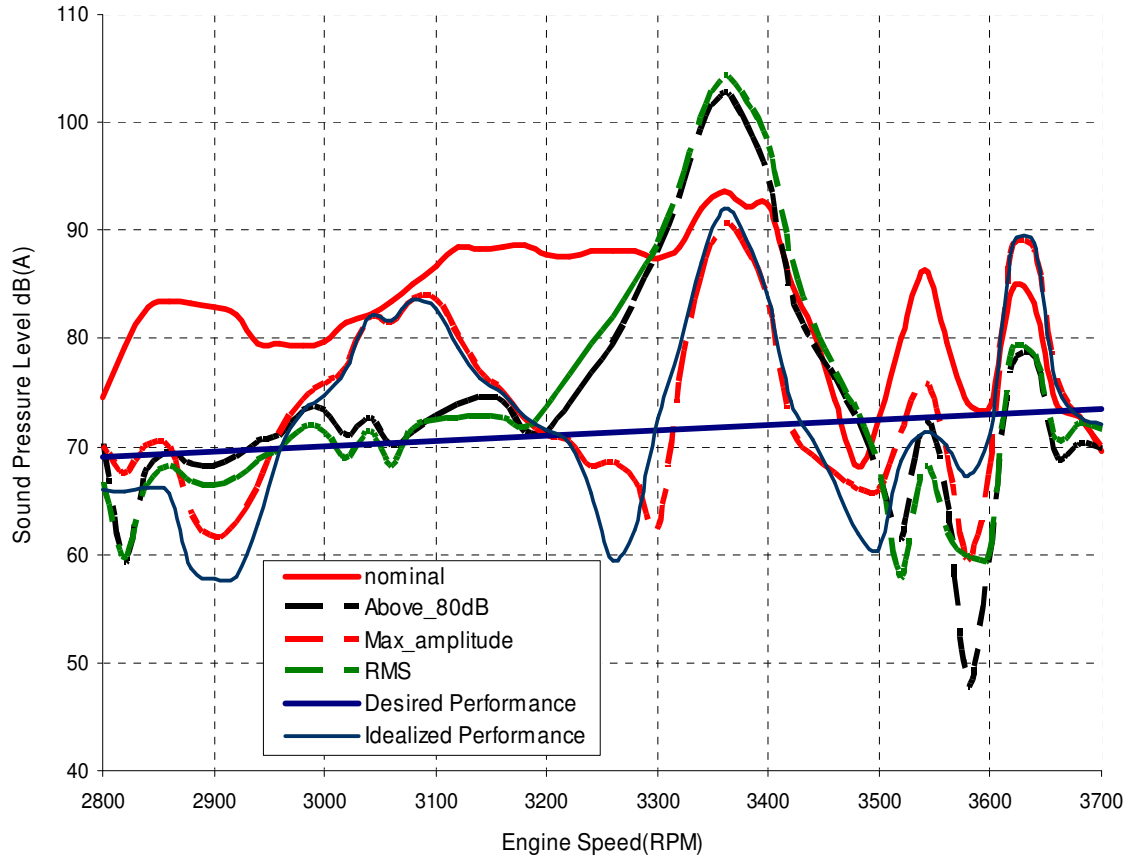
Figure 4.6. Comparison of the optimized configuration results

Figure 4.7 compares the results of the optimized configurations based on the "Idealized Performance" metric with ±10% and ±20:% variation of the front panel thickness.
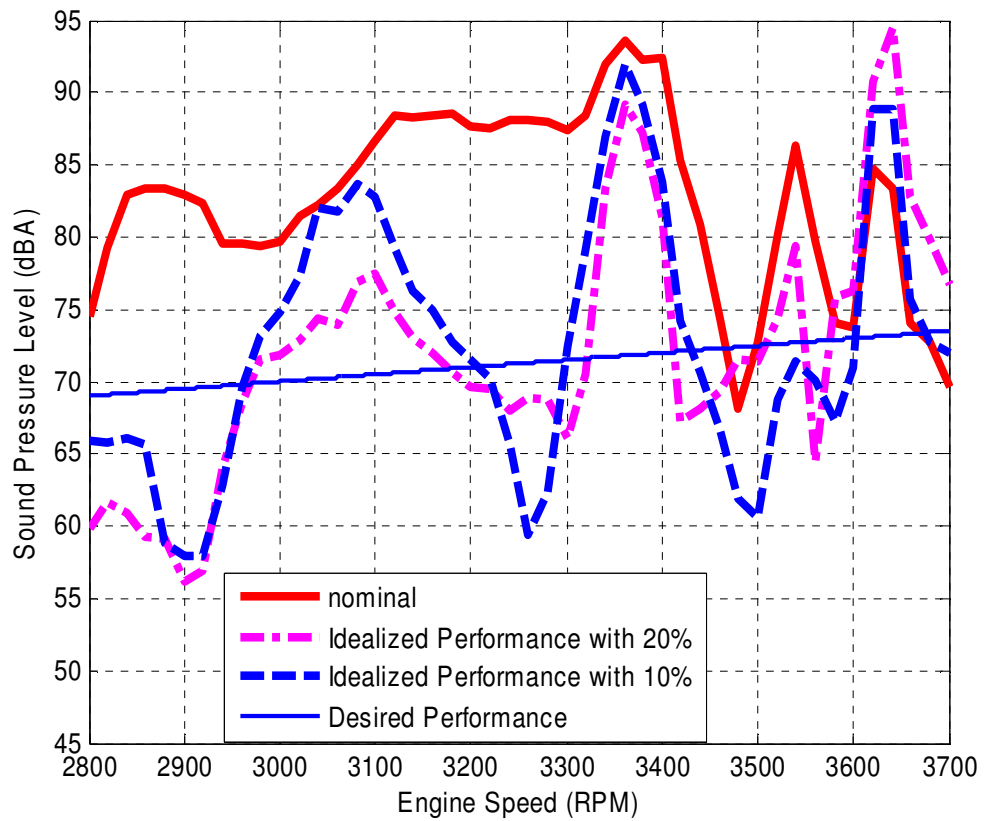
Figure 4.7. Comparison of the optimized configuration results with ±10% and ±20% variation in the front panel thickness

Chapter 5

DISCUSSION AND CONCLUSION

In this study, we developed a methodology to predict and also improve the structure-borne noise caused by the vibrating panels enclosing the vehicle. A vibro-acoustic model of a commercial vehicle was used as the basis for the studies conducted in this thesis.

We adopted a combined use of FEM and BEM methodologies in order to predict the sound pressure level inside the passenger cabin of a commercial vehicle. We used FEM for the structural analysis and BEM for the acoustic analysis. The adopted FEM-BEM approach takes advantage of the Acoustic Transfer Vectors (ATV) to calculate the sound pressure levels at the predefined locations as a function of engine speed. ATVs are transfer functions that link the structural vibrations of the radiating surfaces and the sound pressure levels at the desired output field points. The contribution of each radiating panel to the interior noise is calculated using Panel Acoustic Contribution Analysis (PACA). PACA takes advantage of the ATVs and enables the user to identify the most critical radiating panels. This information can then be utilized to reduce the cabin noise by focusing on these critical panels.

Although the results of the PACA contains a lot of useful information, it does not provide any guidance to the designer regarding how these panels should be modified so that the sound pressure levels can be reduced. The PACA results are only based on the current design and they do not provide any information regarding how the performance changes if any or all of these panel design variables are changed within a certain range. The vehicle contains many structural panels and consequently, there are many design variables that should be looked at when a redesign effort is considered. Especially, when the coupling between the structure and cavity and the interactions between the panels are considered, the reduction of sound pressure level forms a highly non-linear optimization problem, and hence is still considered to be a complicated task even for a simple vibro-acoustic problem.

In this study, we employ techniques from the fields of Design of Experiments (DOE) to understand the relationship between the studied design parameters and sound pressure level. The PACA results are chosen as the basis for the DOE study. The thicknesses of the same panels used in the PACA are used in a DOE study to identify the important ones. Following the DOE analysis, response surface models are built to be used for the optimization studies. Preliminary optimization studies are employed to find the optimum configuration of the panel thicknesses to improve the sound pressure levels based on the selected performance metrics. The metrics selected for this study are *"Percentage*

over 80dBA" Metric, "Max Amplitude" Metric, "Idealized Performance Error" Metric, and "RMS Metric". The front panel thickness was found to be the most influential design variable among the other panel thicknesses included in this study. However, its contribution significantly changed based on the performance metric selected for the analysis. Our study show that the performance metric selection is also very critical in terms of defining the optimum solution and and also finding the optimum configuration. Our results show that the methodology developed in this study can be effectively used for improving the design of the panels to reduce interior noise when the vibro-acoustic response is chosen as the performance criteria.

Our study so far does not consider various constraints on design variables (such as performance requirements, design parameter constraints, etc.). These constraints can be integrated into the optimization procedure. Stochastic models can be integrated to the current method to represent the uncertainties and variations in the design variables due to aging, manufacturability, operating conditions and external disturbances. Also, other multi-objective optimization techniques will be investigated to optimize the current system to investigate better set of optimum solutions for the design parameters.

BIBLIOGRAPHY

[1]I. L. Ver and L. L. Beranek, Noise and Vibration Control Engineering: Principles and Applications, Wiley, 2006.

[2] Lalor, N. and Priebsch, H-H., "The prediction of low- and mid-frequency internal road vehicle noise: a literature survey." J. Automobil Engineering, 221, 245-269, 2007

[3] Suzuki S, Maruyama S, Ido H. "Boundary element analysis of cavity noise problems with complicated boundary conditions." J Sound and Vibr, 130(1), 79–91, 1989.

[4] G. Kamci, I. Basdogan, "Vibro-Acoustic Modeling of a Commercial Vehicle to Reduce the Interior Noise Level", 2009.

[5] Pal C, Hagiwara I., "Dynamic analysis of a coupled structural-acoustic problem. Simultaneous multimodal reduction of vehicle interior noise level by combined optimization." Finite Elements Anal Des, 14, 225–34, 1993.

[6] Liu, Z. S., Lu, C., Wang, Y. Y., Lee, H. P., Koh, Y. K., Lee, K. S. "Prediction of noise inside tracked vehicle." J Applied Acoustics, 64, 74-91, 2006.

[7] Kim S.H., Lee J.M., and Sung M. H., "Structural-Acoustic Model Coupling Analysis and Application to Noise Prediction in a Vehicle Passenger Compartment" Journal of Sound and Vibration, 225(5), 989-999, 1999.

[8] Kim S.H., and Lee J.M., "A Practical Method for Noise Reduction of a Vehicle

Passenger Compartment" Journal of Vibration and Acoustics, 120,199-205, 1998.

[9] Freymann R, Stryczek R, Spannheimer H. "Dynamic response of coupled structuralacoustic systems." J. Low Frequency Noise Vibr, 14(1), 11–32, 1995.

[10] Pal C, Hagiwara I., "Dynamic analysis of a coupled structural-acoustic problem. Simultaneous multimodal reduction of vehicle interior noise level by combined optimization." Finite Elements Anal Des, 14, 225–34, 1993.

[11] Marburg S, Hardtke HJ., "A study on the acoustic boundary admittance. Determination, results and consequences." Eng Anal Boundary Elements, 23, 737–44, 1999.

[12] Marburg S, Hardtke H-J., "Shape optimization of a vehicle hat-shelf: improving acoustic properties for different load cases by maximizing first eigenfrequency." Comput Struct., 79(20–21), 1943–57, 2001.

[13] Marburg S, Beer H-J, Gier J, Hardtke H-J. "Experimental verification of structural acoustic modelling and design optimization." J Sound and Vibr, 252(4), 591–615, 2002.

[14] Marburg S. "Efficient optimization of a noise transfer function by modification of shell structure geometry – Part I: Theory." Struct Multidisciplinary Optim, 24(1), 51–9, 2002.

[15] Marburg S, Hardtke H-J. "Efficient optimization of a noise transfer function by modification of shell structure geometry – Part II: Application to a vehicle dashboard."

Struct Multidisciplinary Optim., 24(1), 60–71, 2002

[16] Bregant, L., Miccoli, G., Seppi, M. "Construction machinery cab vibro-acoustic analysis and optimization, http://www.femtools.com/download/docs/nafems05c.pdf

[17] Desmet W., and Vandepitte D., "Finite Element Modeling for Acoustics" LMS Numerical Acoustics Theoretical Manual, 37-85.

Bibliography 79

[18] Desmet W., "Boundary Element Modeling for Acoustics" LMS Numerical Acoustics Theoretical Manual, 86-126.

[19] Herrin D. W., Martinus F., and Seybert A. F., "Using Numerical Acoustics to Diagnose Noise Problems" SAE Technical Paper Series, 2005-01-2324.

[20] R. A. Fisher, *Statistical Methods for Research Workers,* Oliver and Boyd, Edinburgh, 1958.

[21] D. C. Montgomery, *Design and Analysis of Experiments,* 6th Edition, Wiley, 2005

[22] R. H. Myers and D. C. Montgomery, *Response Surface Methodology, Process and Product Optimization Using Designed Experiments, (2nd Ed.)*, John Wiley and Sons, New York, NY, 2002.

[23] R. H. Myers, D. C. Montgomery, G. G. Vining, C. M. Borror, S. M. Kowalski, Response Surface Methodology: A Retrospective and Literature Survey, *Journal of Quality Technology*, 36(1), 53-77, 2004.

[24] X. Liang, Z. Li., P. Zhu, Acoustic analysis of damping structure with response surface

method, *Applied Acoustics* 68, 1036–1053, 2007.

[25] Z. Li and X. Liang, Vibro-acoustic analysis and optimization of damping structure with Response Surface Method, *Materials and Design* 28, 1999–2007, 2007.

[26] G. Kamci, I. Basdogan, A. Gel, E. S. Gel, A. Koyuncu, and I. Yilmaz, "Vibro-Acoustic Analysis of a Commercial Vehicle Integrated with Design of Experiments Methodology", *Proceedings of 8th World Congress on Structural and Multidisciplinary Optimization*, Lisbon, Portugal, June, 2009.

[27] Papalambros P.Y., Wilde D.J.: *Principles of Optimal Design*, Cambridge University Press, 2000

[28] S. Donders, H. Van der Auweraer, *Engineering Approach for Robust Vibro-Acoustic Design Optimization,* LMS International.

[29] Ralph W. Pike, *Optimization for Engineering Systems*, Chemical Engineering and Systems Science, Louisiana State University, http://www.mpri.lsu.edu/bookindex.html, 2006.

APPENDIX

Table A.1: Results of the full factorial DOE for the *"Percentage over 80 dBA", "Max Amplitude", "RMS" and "Idealized Performance"* metrics.

Exp	bulkhead	frontfloor	backfloor	frontpanel	roof	window	doors	percentage over 80 dB(A)	Max Amplitude	RMS	Idealized Performance
1	0,72	0,72	0,81	0,72	0,63	4,5	0,9	30,434783	102,522042	72,251267	116,5433
2	0,72	0,72	0,81	0,72	0,63	4,5	1,1	30,434783	97,50954583	75,873169	136,08265
3	0,72	0,72	0,81	0,72	0,63	5,5	0,9	28,26087	101,595995	76,671387	74,151491
4	0,72	0,72	0,81	0,72	0,63	5,5	1,1	26,086957	97,56910256	75,243404	135,31579
5	0,72	0,72	0,81	0,72	0,77	4,5	0,9	28,26087	101,7701939	76,541754	78,116472
6	0,72	0,72	0,81	0,72	0,77	4,5	1,1	26,086957	97,49472014	75,346101	120,05383
7	0,72	0,72	0,81	0,72	0,77	5,5	0,9	26,086957	101,8304162	77,439827	86,21404
8	0,72	0,72	0,81	0,72	0,77	5,5	1,1	28,26087	97,5355288	74,557034	120,32769
9	0,72	0,72	0,81	0,88	0,63	4,5	0,9	65,217391	101,9611801	77,256405	294,73768
10	0,72	0,72	0,81	0,88	0,63	4,5	1,1	67,391304	107,9344618	85,921676	377,80953
11	0,72	0,72	0,81	0,88	0,63	5,5	0,9	65,217391	115,6103537	87,831864	286,2719
12	0,72	0,72	0,81	0,88	0,63	5,5	1,1	67,391304	107,8606435	85,602378	375,66182
13	0,72	0,72	0,81	0,88	0,77	4,5	0,9	63,043478	115,8211958	87,699933	300,93986
14	0,72	0,72	0,81	0,88	0,77	4,5	1,1	65,217391	107,8952552	85,838959	374,66608
15	0,72	0,72	0,81	0,88	0,77	5,5	0,9	63,043478	115,90587	87,531969	288,9126
16	0,72	0,72	0,81	0,88	0,77	5,5	1,1	65,217391	107,794638	85,677385	373,56572
17	0,72	0,72	0,99	0,72	0,63	4,5	0,9	28,26087	116,0417301	87,509753	63,495948
18	0,72	0,72	0,99	0,72	0,63	4,5	1,1	32,608696	96,82888653	75,800181	121,68754
19	0,72	0,72	0,99	0,72	0,63	5,5	0,9	30,434783	101,6114637	78,255287	102,03828
20	0,72	0,72	0,99	0,72	0,63	5,5	1,1	30,434783	96,58728654	74,920272	119,11867
21	0,72	0,72	0,99	0,72	0,77	4,5	0,9	28,26087	101,7428186	78,195599	64,925604
22	0,72	0,72	0,99	0,72	0,77	4,5	1,1	30,434783	96,52344085	75,527812	127,3877
23	0,72	0,72	0,99	0,72	0,77	5,5	0,9	30,434783	101,8412304	77,8681	76,441457
24	0,72	0,72	0,99	0,72	0,77	5,5	1,1	30,434783	96,43367132	74,971518	137,40043
25	0,72	0,72	0,99	0,88	0,63	4,5	0,9	65,217391	102,0768706	77,424709	308,21502
26	0,72	0,72	0,99	0,88	0,63	4,5	1,1	63,043478	107,8024624	86,0442	349,26327
27	0,72	0,72	0,99	0,88	0,63	5,5	0,9	69,565217	116,1109678	86,709807	307,39197
28	0,72	0,72	0,99	0,88	0,63	5,5	1,1	60,869565	107,7637457	85,883372	346,00125
29	0,72	0,72	0,99	0,88	0,77	4,5	0,9	67,391304	116,1991335	86,654254	332,41352

30	0,72	0,72	0,99	0,88	0,77	4,5	1,1	58,695652	107,80657	85,990487	345,00236
31	0,72	0,72	0,99	0,88	0,77	5,5	0,9	69,565217	116,2574569	86,439888	310,6996
32	0,72	0,72	0,99	0,88	0,77	5,5	1,1	54,347826	107,7216563	86,029905	343,94033
33	0,72	0,88	0,81	0,72	0,63	4,5	0,9	21,73913	116,2821248	86,51234	66,316466
34	0,72	0,88	0,81	0,72	0,63	4,5	1,1	23,913044	92,19518411	73,018374	109,92075
35	0,72	0,88	0,81	0,72	0,63	5,5	0,9	21,73913	102,0404608	75,153669	67,315276
36	0,72	0,88	0,81	0,72	0,63	5,5	1,1	21,73913	92,05302867	72,512366	110,00547
37	0,72	0,88	0,81	0,72	0,77	4,5	0,9	21,73913	102,2655462	75,064244	74,809184
38	0,72	0,88	0,81	0,72	0,77	4,5	1,1	23,913044	91,93603085	72,625294	108,7491
39	0,72	0,88	0,81	0,72	0,77	5,5	0,9	21,73913	102,3648056	75,769674	84,08529
40	0,72	0,88	0,81	0,72	0,77	5,5	1,1	21,73913	91,8139848	71,797438	112,197
41	0,72	0,88	0,81	0,88	0,63	4,5	0,9	69,565217	102,5221649	75,409895	296,93912
42	0,72	0,88	0,81	0,88	0,63	4,5	1,1	67,391304	105,2558094	86,003291	387,71268
43	0,72	0,88	0,81	0,88	0,63	5,5	0,9	69,565217	113,4200397	87,797564	288,1495
44	0,72	0,88	0,81	0,88	0,63	5,5	1,1	67,391304	105,4419235	86,055103	386,70836
45	0,72	0,88	0,81	0,88	0,77	4,5	0,9	69,565217	113,7386975	87,443345	298,34049
46	0,72	0,88	0,81	0,88	0,77	4,5	1,1	65,217391	105,3451496	86,312905	387,22651
47	0,72	0,88	0,81	0,88	0,77	5,5	0,9	69,565217	113,8459064	87,539715	291,97711
48	0,72	0,88	0,81	0,88	0,77	5,5	1,1	65,217391	105,4844589	86,100309	388,43616
49	0,72	0,88	0,99	0,72	0,63	4,5	0,9	21,73913	114,1273511	87,150004	67,873487
50	0,72	0,88	0,99	0,72	0,63	4,5	1,1	21,73913	90,02832692	73,054938	114,78886
51	0,72	0,88	0,99	0,72	0,63	5,5	0,9	21,73913	102,3260659	75,497039	63,9522
52	0,72	0,88	0,99	0,72	0,63	5,5	1,1	17,391304	89,9117258	72,986314	116,55024
53	0,72	0,88	0,99	0,72	0,77	4,5	0,9	21,73913	102,5479936	75,362817	71,313387
54	0,72	0,88	0,99	0,72	0,77	4,5	1,1	19,565217	89,78562583	72,739911	116,47434
55	0,72	0,88	0,99	0,72	0,77	5,5	0,9	21,73913	102,6326375	75,648341	73,885154
56	0,72	0,88	0,99	0,72	0,77	5,5	1,1	17,391304	89,73406378	72,237297	119,60779
57	0,72	0,88	0,99	0,88	0,63	4,5	0,9	69,565217	102,7748507	75,183821	301,92968
58	0,72	0,88	0,99	0,88	0,63	4,5	1,1	67,391304	105,8941954	86,137289	374,13625
59	0,72	0,88	0,99	0,88	0,63	5,5	0,9	69,565217	113,0158304	86,357505	295,74357
60	0,72	0,88	0,99	0,88	0,63	5,5	1,1	67,391304	106,1758882	86,009057	373,38661
61	0,72	0,88	0,99	0,88	0,77	4,5	0,9	69,565217	113,3933027	86,185281	306,5198
62	0,72	0,88	0,99	0,88	0,77	4,5	1,1	65,217391	106,0002944	86,182664	373,19346
63	0,72	0,88	0,99	0,88	0,77	5,5	0,9	67,391304	113,4883432	86,145252	298,09496
64	0,72	0,88	0,99	0,88	0,77	5,5	1,1	65,217391	106,1929841	85,92915	375,70593
65	0,88	0,72	0,81	0,72	0,63	4,5	0,9	28,26087	113,8034479	85,993173	70,654827
66	0,88	0,72	0,81	0,72	0,63	4,5	1,1	41,304348	96,7356193	76,394519	160,53819
67	0,88	0,72	0,81	0,72	0,63	5,5	0,9	28,26087	104,9308443	78,317591	69,920572

68	0,88	0,72	0,81	0,72	0,63	5,5	1,1	39,130435	96,77146396	76,240359	158,2436
69	0,88	0,72	0,81	0,72	0,77	4,5	0,9	30,434783	105,3571613	78,524859	77,510765
70	0,88	0,72	0,81	0,72	0,77	4,5	1,1	39,130435	96,78348996	75,704746	152,57812
71	0,88	0,72	0,81	0,72	0,77	5,5	0,9	26,086957	105,1113081	78,735313	80,814166
72	0,88	0,72	0,81	0,72	0,77	5,5	1,1	36,956522	96,67533926	75,46462	155,20858
73	0,88	0,72	0,81	0,88	0,63	4,5	0,9	63,043478	105,4479543	78,716148	271,4361
74	0,88	0,72	0,81	0,88	0,63	4,5	1,1	69,565217	106,4487691	84,954363	407,80358
75	0,88	0,72	0,81	0,88	0,63	5,5	0,9	63,043478	118,1631799	88,521402	269,84533
76	0,88	0,72	0,81	0,88	0,63	5,5	1,1	67,391304	106,2240329	84,446713	404,52048
77	0,88	0,72	0,81	0,88	0,77	4,5	0,9	63,043478	118,3886356	88,220195	273,07034
78	0,88	0,72	0,81	0,88	0,77	4,5	1,1	67,391304	106,4252718	84,961506	403,95661
79	0,88	0,72	0,81	0,88	0,77	5,5	0,9	63,043478	118,2857961	88,063869	272,48026
80	0,88	0,72	0,81	0,88	0,77	5,5	1,1	65,217391	106,167636	84,402346	401,49233
81	0,88	0,72	0,99	0,72	0,63	4,5	0,9	28,26087	118,4232958	87,965089	61,881532
82	0,88	0,72	0,99	0,72	0,63	4,5	1,1	39,130435	95,13929772	76,325525	145,71784
83	0,88	0,72	0,99	0,72	0,63	5,5	0,9	28,26087	103,5724643	79,133228	62,186793
84	0,88	0,72	0,99	0,72	0,63	5,5	1,1	36,956522	95,01419147	76,338564	142,67911
85	0,88	0,72	0,99	0,72	0,77	4,5	0,9	30,434783	104,0710933	79,273808	64,451934
86	0,88	0,72	0,99	0,72	0,77	4,5	1,1	39,130435	95,16529808	76,003106	153,6321
87	0,88	0,72	0,99	0,72	0,77	5,5	0,9	26,086957	103,8911939	78,71054	62,822886
88	0,88	0,72	0,99	0,72	0,77	5,5	1,1	36,956522	95,03522013	75,915361	153,03324
89	0,88	0,72	0,99	0,88	0,63	4,5	0,9	65,217391	104,3221365	78,598817	295,24071
90	0,88	0,72	0,99	0,88	0,63	4,5	1,1	65,217391	107,0629515	85,082148	383,61611
91	0,88	0,72	0,99	0,88	0,63	5,5	0,9	67,391304	117,9403058	87,29016	291,90777
92	0,88	0,72	0,99	0,88	0,63	5,5	1,1	65,217391	106,8659315	84,539967	380,14254
93	0,88	0,72	0,99	0,88	0,77	4,5	0,9	67,391304	118,2060793	86,986959	307,05695
94	0,88	0,72	0,99	0,88	0,77	4,5	1,1	60,869565	107,1201007	84,886188	379,09141
95	0,88	0,72	0,99	0,88	0,77	5,5	0,9	67,391304	118,146087	86,889866	299,54836
96	0,88	0,72	0,99	0,88	0,77	5,5	1,1	58,695652	106,8884785	84,482278	376,61132
97	0,88	0,88	0,81	0,72	0,63	4,5	0,9	21,73913	118,3305011	86,745494	79,641496
98	0,88	0,88	0,81	0,72	0,63	4,5	1,1	26,086957	91,67137951	73,221413	151,11702
99	0,88	0,88	0,81	0,72	0,63	5,5	0,9	21,73913	104,6779632	75,341067	78,311703
100	0,88	0,88	0,81	0,72	0,63	5,5	1,1	26,086957	91,54077862	72,975536	137,01811
101	0,88	0,88	0,81	0,72	0,77	4,5	0,9	21,73913	105,0399068	75,608405	106,07348
102	0,88	0,88	0,81	0,72	0,77	4,5	1,1	26,086957	91,61299105	72,596979	140,38464
103	0,88	0,88	0,81	0,72	0,77	5,5	0,9	21,73913	104,8906835	75,809662	106,98733
104	0,88	0,88	0,81	0,72	0,77	5,5	1,1	26,086957	91,52823502	72,02894	142,49691
105	0,88	0,88	0,81	0,88	0,63	4,5	0,9	65,217391	105,155565	75,555476	257,04649

|											
106	0,88	0,88	0,81	0,88	0,63	4,5	1,1	67,391304	105,8019195	84,629665	420,27254
107	0,88	0,88	0,81	0,88	0,63	5,5	0,9	67,391304	116,1237254	87,784053	250,02756
108	0,88	0,88	0,81	0,88	0,63	5,5	1,1	67,391304	105,877806	84,45887	419,45312
109	0,88	0,88	0,81	0,88	0,77	4,5	0,9	67,391304	116,5591037	87,535532	262,22661
110	0,88	0,88	0,81	0,88	0,77	4,5	1,1	65,217391	105,832237	84,812569	421,5829
111	0,88	0,88	0,81	0,88	0,77	5,5	0,9	65,217391	116,4020173	87,43636	253,69701
112	0,88	0,88	0,81	0,88	0,77	5,5	1,1	65,217391	105,8537036	84,512718	417,15627
113	0,88	0,88	0,99	0,72	0,63	4,5	0,9	23,913044	116,7547192	87,293759	62,691902
114	0,88	0,88	0,99	0,72	0,63	4,5	1,1	26,086957	90,58896479	73,832872	149,23443
115	0,88	0,88	0,99	0,72	0,63	5,5	0,9	21,73913	103,5921196	75,49943	66,522893
116	0,88	0,88	0,99	0,72	0,63	5,5	1,1	21,73913	90,52604743	73,540738	128,29421
117	0,88	0,88	0,99	0,72	0,77	4,5	0,9	23,913044	104,0254273	75,72972	66,918651
118	0,88	0,88	0,99	0,72	0,77	4,5	1,1	23,913044	90,71972078	73,483172	135,52368
119	0,88	0,88	0,99	0,72	0,77	5,5	0,9	21,73913	103,8972557	75,628506	72,625378
120	0,88	0,88	0,99	0,72	0,77	5,5	1,1	21,73913	90,68569887	72,804654	128,88934
121	0,88	0,88	0,99	0,88	0,63	4,5	0,9	63,043478	104,225522	75,455452	289,79058
122	0,88	0,88	0,99	0,88	0,63	4,5	1,1	67,391304	107,3261933	84,772124	402,37677
123	0,88	0,88	0,99	0,88	0,63	5,5	0,9	63,043478	115,2690216	87,012893	274,88285
124	0,88	0,88	0,99	0,88	0,63	5,5	1,1	65,217391	107,4625018	84,76193	426,08246
125	0,88	0,88	0,99	0,88	0,77	4,5	0,9	63,043478	115,7040031	86,623814	288,52948
126	0,88	0,88	0,99	0,88	0,77	4,5	1,1	65,217391	107,3135349	85,070752	427,55875
127	0,88	0,88	0,99	0,88	0,77	5,5	0,9	63,043478	115,611961	86,411858	277,01362
128	0,88	0,88	0,99	0,88	0,77	5,5	1,1	63,043478	107,3819879	84,81185	409,95852
129	0,8	0,8	0,9	0,8	0,7	5	1	67,391304	93,973792	86,514594	173,12087
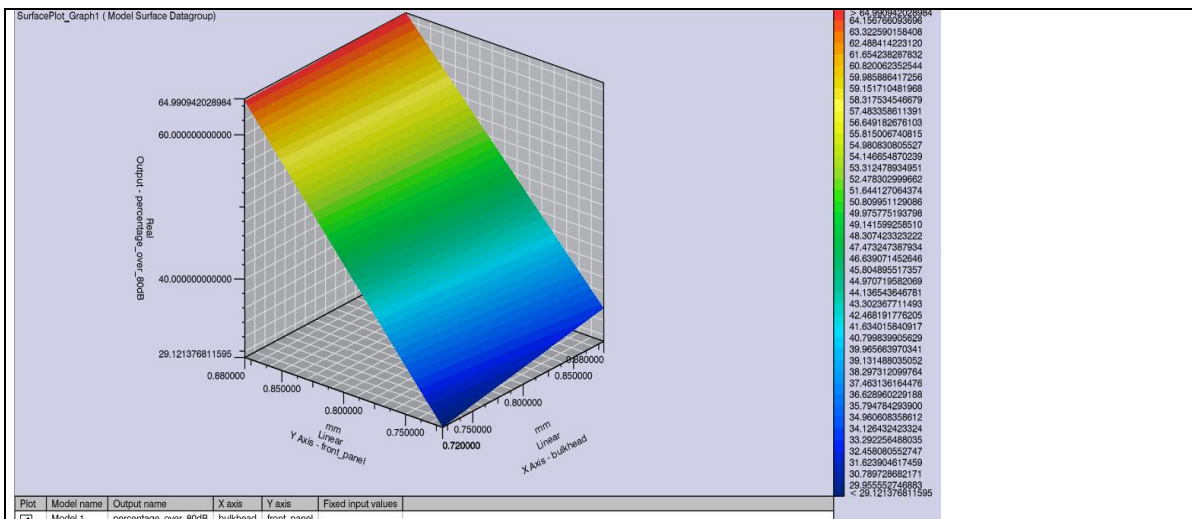
Figure A.1.1: Modal Surface Plot for the metric "*Above 80dB(A)*". The bulkhead panel constitutes the y axis and the Front panel constitutes the x axis. The output parameter which is the z axis has the values between 29.12 and 64.99 within the 10% change of the bulkhead and front panel thickness
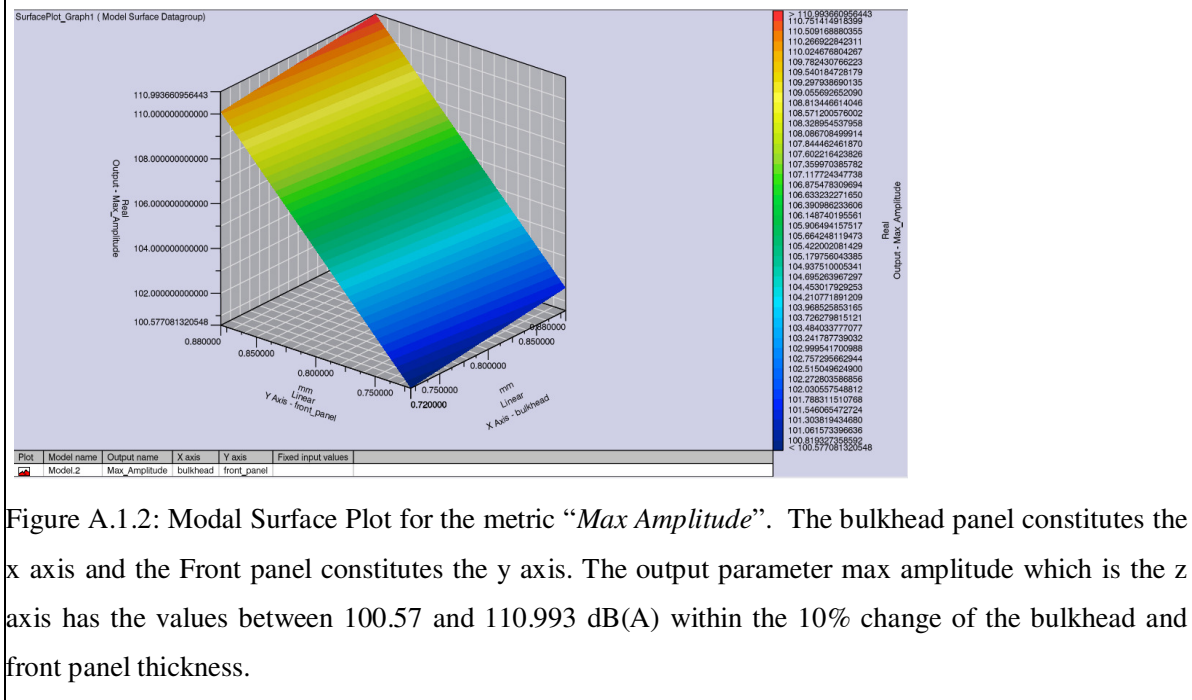

Figure A.1.2: Modal Surface Plot for the metric "*Max Amplitude*". The bulkhead panel constitutes the x axis and the Front panel constitutes the y axis. The output parameter max amplitude which is the z axis has the values between 100.57 and 110.993 dB(A) within the 10% change of the bulkhead and front panel thickness.

Figure A.1: Modal Surface plots for the metrics : "*Above 80dB(A)*" and" *Max Amplitude*."
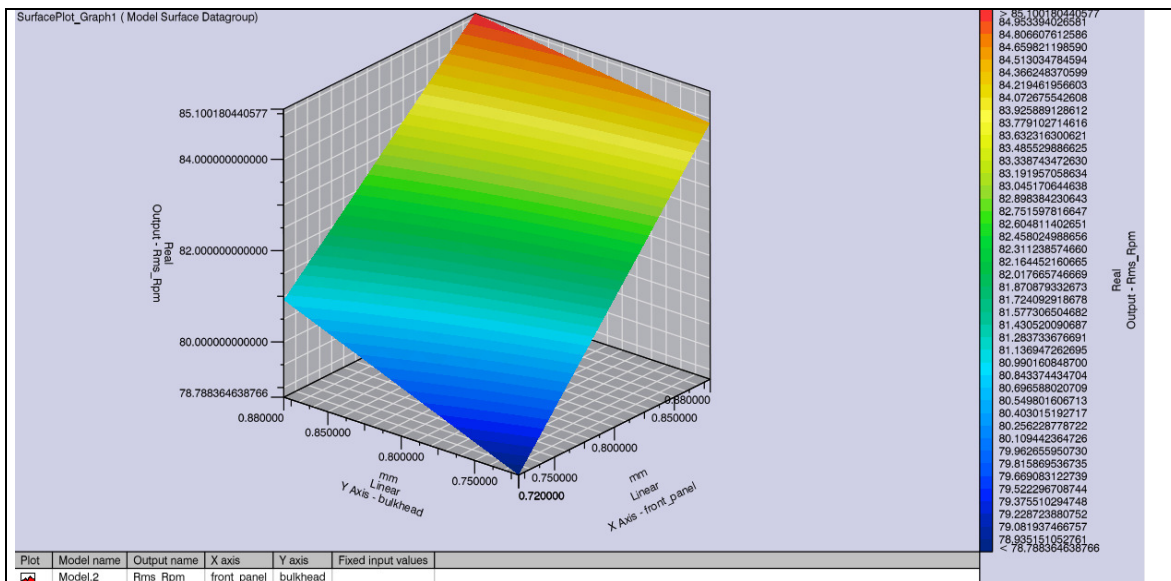
Figure 4.10.1: Modal Surface Plot for the metric "*RMS*". The bulkhead panel constitutes the y axis and the front panel constitutes the x axis. The output parameter rms which is the z axis has the values between 76.78 and 85.100 within the 10% change of the bulkhead and front panel thickness
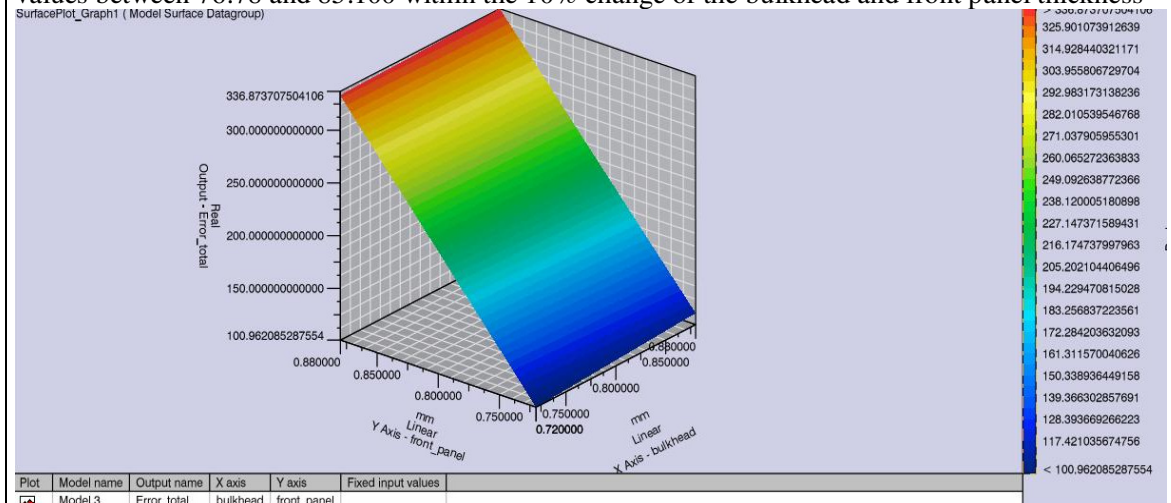

Figure 4.10.2: Modal Surface Plot for the parameter "*Idealized Performance*". The bulkhead panel constitutes the x axis and the Front panel constitutes the y axis. The output parameter Total error amplitude which is the z axis has the values between 100.57 and 110.993 within the 10% change of the bulkhead and front panel thickness

Figure A.2: Modal Surface plot for the metrics: "*RMS*" and "*Idealized Performance*".
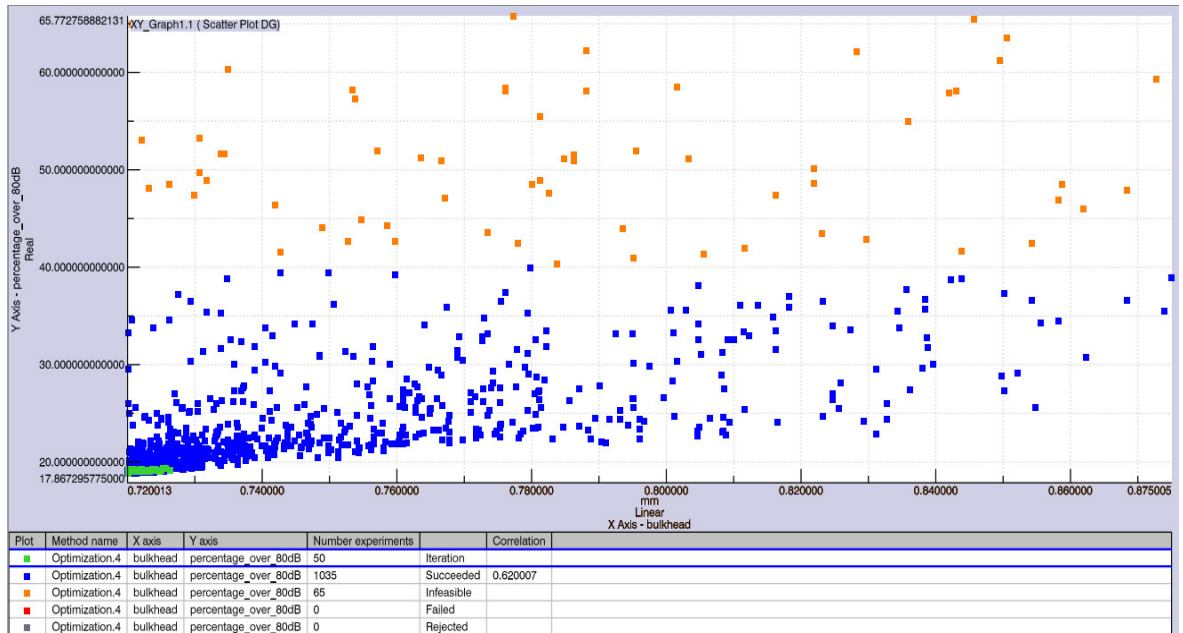
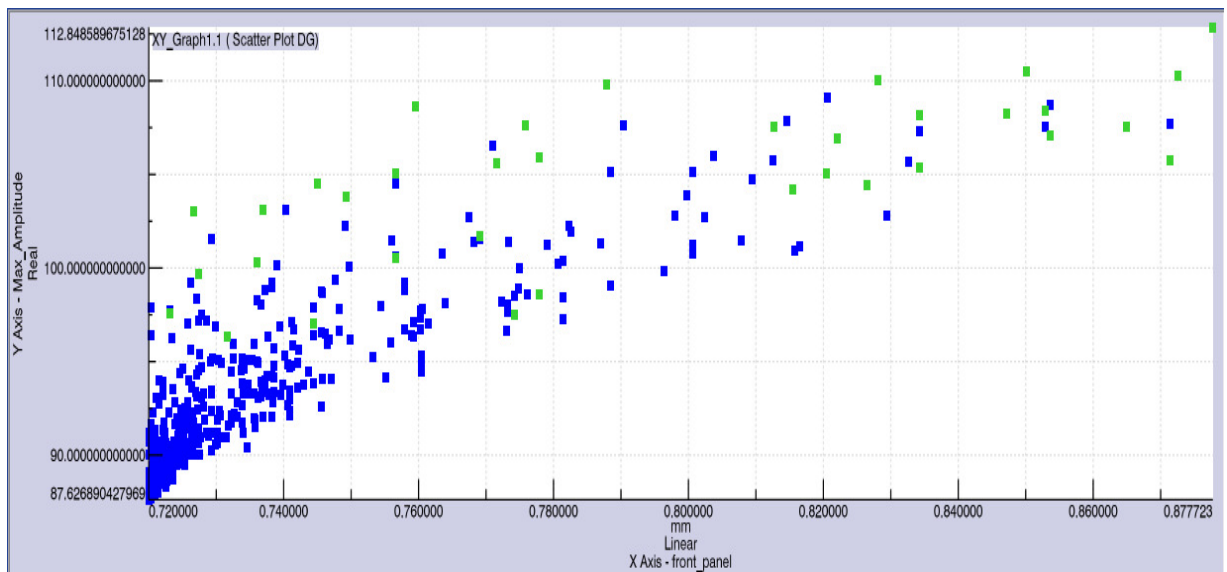Figure A.3: optimization scatter plot for the 1035 iterations for the metric "*Percentage over 80 dBA*".

Figure A.4: optimization scatter plot for the 1035 iterations for the metric "*Max Amplitude*".